REPORT DOCUMENTATION PAGE

1. Report No.	2.	3. Recipient's Accession No.

4. Title and Subtitle	5. Report Date
Experiments on the Erosion of Deposited and Placed Cohesive Sediments in an Annular Flume and a Rocking Flume	June, 1986
	6.

7. Author(s)	8. Performing Organization Report No.
Catherine Villaret Mary Paulic	UFL/COEL-86/007

9. Performing Organization Name and Address	10. Project/Task/Work Unit No.
Coastal and Oceanographic Engineering Department University of Florida 336 Weil Hall Gainesville, FL 32611	11. Contract or Grant No. DACW39-84-C-0013
12. Sponsoring Organization Name and Address U.S. Army Engineer Waterways Experiment Station P.O. Box 631 Vicksburg, MS 39180	13. Type of Report
	14.

15. Supplementary Notes

16. Abstract

The effects of bed structure and flow regime on the erosional behavior of fine, cohesive sediments were investigated in a series of laboratory experiments. Two types of beds, placed and deposited, were used in both a rotating annular flume under a constant shear stress, τ_b, and in a rocking flume under an oscillatory shear stress. The deposited bed represents the top sediment layers of an estuarine bed which is frequently resuspended by the action of currents and waves. In the flumes they were formed by allowing a dilute suspension of sediment to settle out of the water column and consolidate into a bed. The placed bed represents those layers of the estuarine bed which are not regularly perturbed; thus they have had time to consolidate. They were prepared as a dense slurry and then placed into the apparatus. A commercial kaolinite, and estuarine sediments collected from a tidal mud flat in Cedar Key, Florida and from San Francisco Bay, were used to prepare the beds.

Kaolinite and Cedar Key Mud: Comparative analyses of the results from both types of beds yielded distinct concentration-time profiles and different relationships for the rate of erosion as a function of excess shear stress, $\tau_b - \tau_s$, above the bed shear strength, τ_s. The deposited beds yielded a concentration-time profile representing a succession of steady states. The placed beds yielded a linear profile. The difference in profiles is best explained by corresponding differences in the vertical distribution of bed shear strength.

- Continued -

17. Originator's Key Words		18. Availability Statement
Annular flume	Erosion rate	
Cedar Key mud	Kaolinite	
Cohesive sediment	Rocking flume	
Critical shear stress	San Francisco Bay mud	

19. U. S. Security Classif. of the Report	20. U. S. Security Classif. of This Page	21. No. of Pages	22. Price
Unclassified	Unclassified	61	

The relationship between the mass rate of erosion, ε, and excess shear stress was found to be approximated by $\log(\varepsilon/\varepsilon_f) = \alpha[\tau_b - \tau_s(z)]^{1/2}$ for the deposited bed, and $\varepsilon = M(\tau_b - \tau_s)/\tau_s$ for the placed bed, where z is depth below the bed surface. The coefficients ε_f (floc erosion rate), α and M were, in general, not the same for the two flumes; they were higher under oscillatory current in the rocking flume than under uni-directional current in the annular flume. Sediment type, bed structure and current regime are important factors in determining the erosional behavior of a cohesive sediment.

San Francisco Bay Mud: An erosion rate expression was found relating the rate of erosion to the bulk density of the bed and the current speed. Bed density was found to be a strong influential parameter. Soft beds (1.2 g/cm^3 density) generally showed a significantly higher rate of erosion than dense beds (~ 1.6 g/cm^3) at the same current speed.

UFL/COEL-86/007

EXPERIMENTS ON THE EROSION OF DEPOSITED AND PLACED COHESIVE SEDIMENTS IN AN ANNULAR FLUME AND A ROCKING FLUME

by

Catherine Villaret

Mary Paulic

Coastal and Oceanographic Engineering Department

University of Florida

Gainesville, FL 32611

June, 1986

FOREWORD

The methodology for the reported erosion studies is based on laboratory experimental procedures developed previously at the University of Florida. For details, which have been omitted here, the reader should refer to Parchure and Mehta (1985), who used the annular flume with flow deposited beds. Results using placed beds in the annular flume are being reported here for the first time. Likewise, the rocking flume was used for the first time in this study. This flume was designed under a previous project supported by the Florida Sea Grant College, NOAA, through Grant IR-84-25. Drs. C. Montague and A. J. Mehta were the principal investigators. The present study was supported by the U.S. Army Engineer Waterways Experiment Station, Vicksburg, MS, Contract No. DACW39-84-C-0013. Dr. A. J. Mehta was the principal investigator. Support through both agencies is sincerely acknowledged.

TABLE OF CONTENTS

TABLE OF CONTENTS

(Continued)

LIST OF FIGURES

LIST OF FIGURES

(Continued)

LIST OF FIGURES

(Continued)

LIST OF TABLES

ABSTRACT

The effects of bed structure and flow regime on the erosional behavior of fine, cohesive sediments were investigated in a series of laboratory experiments. Two types of beds, placed and deposited, were used in both a rotating annular flume under a constant shear stress, τ_b, and in a rocking flume under an oscillatory shear stress. The deposited bed represents the top sediment layers of an estuarine bed which is frequently resuspended by the action of currents and waves. In the flumes they were formed by allowing a dilute suspension of sediment to settle out of the water column and consolidate into a bed. The placed bed represents those layers of the estuarine bed which are not regularly perturbed; thus they have had time to consolidate. They were prepared as a dense slurry and then placed into the apparatus. A commercial kaolinite, and estuarine sediments collected from a tidal mud flat in Cedar Key, Florida and from San Francisco Bay, were used to prepare the beds.

Kaolinite and Cedar Key Mud: Comparative analyses of the results from both types of beds yielded distinct concentration-time profiles and different relationships for the rate of erosion as a function of excess shear stress, $\tau_b-\tau_s$, above the bed shear strength, τ_s. The deposited beds yielded a concentration-time profile representing a succession of steady states. The placed beds yielded a linear profile. The difference in profiles is best explained by corresponding differences in the vertical distribution of bed shear strength.

The relationship between the mass rate of erosion, ε, and excess shear stress was found to be approximated by $\log(\varepsilon/\varepsilon_f) = \alpha[\tau_b-\tau_s(z)]^{1/2}$ for the deposited bed, and $\varepsilon=M(\tau_b-\tau_s)/\tau_s$ for the placed bed, where z is depth below the bed surface. The coefficients ε_f (floc erosion rate), α and M were, in general, not the same for the two flumes; they were higher under oscillatory current in the rocking flume than under uni-directional current in the annular flume. Sediment type, bed structure and current regime are important factors in determining the erosional behavior of a cohesive sediment.

San Francisco Bay Mud: An erosion rate expression was found relating the rate of erosion to the bulk density of the bed and the current speed. Bed density

was found to be a strong influential parameter. Soft beds (1.2 g/cm^3 density) generally showed a significantly higher rate of erosion than dense beds (~ 1.6 g/cm^3) at the same current speed.

PART 1. KAOLINITE AND CEDAR KEY MUD

I. INTRODUCTION

The erosion of fine, cohesive sediments in estuaries is important to both the engineer and the scientist. The resuspension and transport of fine sediments can cause shoaling in ship channels resulting in increased time and cost of dredging. From an environmental perspective, resuspension of sediment increases turbidity, thus degrading water quality and possibly harming aquatic organisms.

Under mild to moderate flow conditions in the estuary, erosion of the mud surface typically occurs by the entrainment of aggregates rather than by mass erosion. The erosional behavior of a mud bed depends on four principal factors; physico-chemical properties of the mud, chemical properties of the eroding fluid, flow characteristics, and bed structure (Parchure and Mehta, 1985). Bed structure can be classified as either placed or deposited, in relation to the procedure for bed preparation. For the purposes of this report, a placed bed is defined as one in which the bed has been prepared by placing a thick slurry of mud into the laboratory apparatus. A deposited bed is produced by allowing a dilute mud suspension to settle from the water column and consolidate. The deposited bed represents the top sediment layers of an estuarine sediment which are frequently resuspended by the action of waves and currents. A placed bed is more representative of the lower sediment layers which do not regularly receive perturbations from waves and currents.

The influence of the first three parameters on the erosion rate of cohesive sediments has been extensively studied (Parchure and Mehta, 1985). The majority of laboratory experiments performed have used only one bed structure and flow regime without comparative studies of different bed structures and flow regimes. The main purpose of this study was to show the effect of bed structure on the rate of surface erosion under both steady and oscillatory currents. Two different apparatuses, a rotating annular flume and a rocking flume, were used to generate a steady current and an oscillatory current, respectively. Both bed types, using both kaolinite and estuarine mud, were tested in each apparatus. Table 1 is a list of the experiments performed.

Table 1. Experimental Design

Apparatus	Sediment/Bed	
	Kaolinite	Estuarine Mud
Annular Flume	Deposited bed Placed bed	Deposited bed Placed bed
Rocking Flume	Deposited bed Placed bed	Deposited bed Placed bed

Bed Structure

The primary difference between placed and deposited beds is the distribution of bed shear strength (and density) with depth. A deposited bed shows an increase in shear strength with increasing depth into the bed (Figure 1). This is a Type I profile. Placed beds have a nearly constant shear strength from top to bottom (Figure 2). Such a profile is referred to as Type II (Parchure, 1984; Hunt and Mehta, 1985).

A profile of density with depth is critical to determining erosion rates. Bed density increases in a deposited bed from top to bottom. On the other hand, a placed bed has nearly uniform density from top to bottom. Deposited beds undergo both primary and secondary consolidation as compared to mainly secondary consolidation for placed beds (Parchure, 1984). Due to their mode of preparation, deposited beds are generally weaker (lower density and shear strength) than placed beds for a comparable period of consolidation.

Concentration-Time Profiles

For a deposited bed the rate of erosion, ε (the time-rate of change of suspended sediment mass per unit bed surface area), which is proportional to the time-rate of change of suspension concentration, decreases as erosion proceeds and eventually stops. Once this steady state condition has been reached, the concentration of suspended mass remains constant, as in Figure 3a. Erosion is no longer occurring. At this stage, the bed shear strength at the mud-fluid interface is equal to the applied shear stress, τ_b.

Placed beds behave differently. The suspended sediment concentration increases linearly with time for a given shear stress in excess of the shear strength, as in Figure 3b. Thus, the rate of erosion of these beds is constant for a given shear stress.

Erosion Rate Expressions

Erosion of a deposited bed can be empirically modeled as a logarithmic relationship correlating the erosion rate to the excess shear stress above the bed shear strength. This relationship is:

$$\log \frac{\varepsilon}{\varepsilon_f} = \alpha[\tau_b - \tau_s(z)]^{1/2} \tag{1}$$

where ε is the erosion rate, τ_b is the time-mean bed shear stress, $\tau_s(z)$ is the bed shear strength as a function of depth, z, below the bed surface, α is an empirical rate constant and ε_f is defined as the floc erosion rate (Parchure, 1984; Parchure and Mehta, 1985).

The erosion rate of a placed bed can be related to the bed shear stress by:

$$\varepsilon = M \frac{(\tau_b - \tau_s)}{\tau_s} \tag{2}$$

where τ_s is the constant (critical) bed shear strength and M is an empirical coefficient (Parchure and Mehta, 1985).

II. METHODS AND MATERIALS

Apparatus

Two different flumes were used for these experiments; a rotating annular flume and a rocking flume.

Annular Flume. The annular flume had a channel width of 20 cm, depth of 46 cm, and a mean radius of 76 cm. Inside the channel a 20 cm plexiglass annular ring was suspended by means of four vertical supports attached by horizontal supports to the central vertical shaft (Figure 4). The equipment was calibrated to produce a bed shear stress up to 0.9 N/m^2. Complete details of flume calibration are contained in Mehta (1973). The total depth of

sediment and water in the flume could be up to 33 cm. For the described experiments a bed of 7 cm depth and water column height of 23 cm were used.

When the ring was rotated, a shear stress was transmitted to the sediment bed through the water column. To operate properly the ring was required to be in complete surface contact with the water column. During operation the ring and channel were rotated in opposite directions to minimize the effects of secondary currents and to maintain a uniform flow in the channel.

Taps were located on the outside wall of the channel to allow sampling from the water column. Samples were collected over a variable time regime. Total suspended sediment was determined by filtering water samples with a 0.45 micron Millipore filter and filtering apparatus. Samples were then dried at 50°C for at least two hours and then weighed on a Mettler balance (model H80) with an accuracy of 0.1 mg.

Rocking Flume. The rocking flume was constructed of 1.25 cm thick plexiglass. It was 2.4 meters in length and 36 cm high with an inner width of 15 cm. A false bottom was built into the flume at a height of 7 cm. The actual depth of the flume channel was therefore 29 cm. Figures 5a, 5b and 6a illustrate plan, elevation and side views of the flume. The entire assembly was mounted on a table with dimensions of 2.75 meters in length, 91 cm in width, and 91 cm in height. The flume was mounted on a pivot 16 cm above the table allowing it freedom of rocking motion. Directly above the pivot the channel had been deepened an additional 5 cm for a length of 54 cm to allow for the placement of a sediment bed. The flume was operated by a hydraulic transmisison attached to a 3/4 hp motor. A metal shaft (rocking arm) at one end of the flume was attached by a circular hub to the flume and to the hydraulic transmission by a hub attached to a rotating plate (Figures 5a,b and 6a). When the flume was in operation, the transmission turned a shaft which turned the rotating plate. This caused the shaft to move up and down resulting in the flume rocking back and forth. Different periods of rocking could be obtained by increasing the speed of the motor and the attached shaft. Amplitude of rocking motion could be varied by changing the eccentricity of the rocking arm/rotating plate connection.

When the flume was operated a standing wave was produced which had its node at the center of the flume, in the middle of the sediment bed. The waves produced were of shallow water type so that the oscillatory velocities were

nearly uniform over depth. Maximum horizontal displacement occurred at the node where the velocity was predominantly in the horizontal direction, along the bed surface. Wave period could be determined by timing the rotation of the plate. Wave amplitude could be determined by measuring the vertical displacement of water from still water level at the end of the flume.

A modification was made to the flume to increase the flow velocity at the bed surface. A plexiglass top constriction of height 19 cm and 54 cm length was placed in the water column above the sediment bed (Figure 6b,c). The ends of it were sloped to reduce turbulence at the entrance to the bed. Its height above the bed could be varied. With the top constriction in place, free surface flow in the flume was thus replaced by flow in a "tunnel" in the central portion of the flume. Over time the current generated at the sediment surface had a sinusoidal velocity variation.

Flume Calibration. The flume was calibrated to produce a maximum shear stress up to 0.8 N/m^2. Maximum shear stress was calculated as $0.5\ \rho f_w u_m^2$, where ρ is water density, f_w is the coefficient of friction, and u_m is the maximum horizontal water velocity. A number of different techniques were used to determine velocity. These included direct measurement of the displacement of the water level relative to the mean, mean surface particle displacement at the node, and velocity of the water above the bed. For these experiments a water depth of 10 cm was maintained above the bed and 17.5 cm at the ends. Complete details, calculations, and calibration curves are contained in the Appendix.

Bed Preparation

Placed Bed. A thick slurry of sediment and salt water (salinity 10 ppt) was mixed for one hour in a mixer and then placed into the flume to uniform depth. Water was then carefully added to the flume to the appropriate depth. A separate bed was placed in a bucket for determination of bed density.

Deposited Bed. An appropriate volume of sediment was added to the annular flume and water added to a depth of 30 cm. The flume was then rotated to generate a bed shear stress of 0.9 N/m^2, in order to assure complete mixing. After 24 hours, the flume was stopped and the sediment allowed to settle under quiescent conditions. After mixing, but before significant

settling of the sediment, water containing suspended sediment was withdrawn from the channel and deposited into removable beds (Figure 6d) that could be placed directly into the rocking flume. The ends of these beds were temporarily sealed with plexiglass to allow a water column to be poured over the bed. A second sample was withdrawn from the annular flume and allowed to deposit in a bucket. This was later used for bed density measurement.

Test Procedure

Annular Flume. For each experiment six different shear stresses were selected. They were applied in a step-wise fashion starting at 0.1 N/m^2 and continuing until 0.6 N/m^2 in increments (90 min duration) of 0.1 N/m^2. Suspension samples were removed, in approximately 50 ml aliquots, at 2,5,10, 15,20,25,30,40,50,60,75, and 90 minutes with an initial sample taken at the start of the test. Samples were taken from taps at the top and bottom of the water column to give an average suspension concentration for the entire water column. Salt water was periodically added to the flume to maintain a 23 cm water depth.

Rocking Flume. Shear stresses selected in this flume were 0.1, 0.2, 0.3, and, in some cases, 0.4 N/m^2. Note that these are wave-averaged rather than maximum values. Samples were collected over the same time regime as for the annular flume, excluding the 2 minute sample. Samples were taken from the center of the flume, at one-quarter reach and at one end, including the top and bottom at each location. Salt water was added periodically to the flume to replace the volume of water lost to samples.

The test procedure with regard to the applied shear stress is summarized in Figure 7 for both flumes. Note that with respect to deposition and consolidation, the duration of deposition was typically quite small compared with that of consolidation. In what follows, the combined duration is referred to as consolidation period.

Materials

Estuarine Sediment. The mud was collected from a tidal flat in Cedar Key, Florida. Mineralogically it was composed of 73% montmorillonite, 21% kaolinite and 6% quartz. Prior to being used, the mud was sieved through a 1 mm screen to remove shells and plant materials. The median (dispersed)

particle size was ~ 2 microns, as obtained by hydrometer (ASTM, 1981). The cation exchange capacity was ≈ 100 millequivalents per hundred grams. Total organic matter corresponded to 11% loss on ignition, as obtained by standard procedure (American Public Health Association, 1976).

Kaolinite. The kaolinite was obtained from a commercial source. It was prepared by soaking 90 kg dry kaolinite in thirty gallons of salt water (salinity 10 ppt) for one month. The kaolinite-water mixture was stirred every few days to ensure equilibration of the sediment with the fluid. The median (dispersed) size was ~ 1 μm. The cation exchange capacity was ~ 6 milliequivalents per hundred grams and loss on ignition was 12%.

Fluid. All experiments were performed with salt water at a salinity of 10 ppt. Salt water was prepared by mixing sodium chloride in tap water. Salinity was checked by a refractometer. Fluid temperature during the tests was in the range of 24°-27°C. The pH varied from 8.5 to 9.5.

Density Measurement

The method used for determining bed density followed the procedure of Parchure (1984). The apparatus used consisted of a 2.0 cm diameter coring tube and a 15 cm diameter plexiglass cylinder with a 2.5 cm diameter metal tube in the middle (Figure 8). Cores were taken from the bed and then the cylinder was placed over the coring tube. The inside of the cylinder was filled with ethanol and dry ice to snap freeze the cores *in situ*. Once frozen the cores were sliced into thin sections between 2 mm and 10 mm, dried at 40°C and weighed.

III. RESULTS

Density Measurement

Deposited Bed. The density of deposited bed typically increases with depth. Such a trend was observed for both kaolinite and estuarine mud. Density (dry) profiles are contained in Figure 9 for kaolinite and Figure 10 for mud.

Placed Bed. The density of a placed bed is fairly constant with depth. Density (dry) profiles are contained in Figure 11 for kaolinite and Figure 12 for mud. The measured values indicate deviations from uniformity with depth.

Concentration-Time Profiles

Deposited Bed. Figures 13 through 16 are plots of suspension concentration versus time. Where deemed important, comments on the observed trends have been made within the figures, e.g. Figure 16. Most comments made here and in subsequent figures are either self-explanatory, or are discussed in the text. The total (instantaneous) suspension concentration is represented as a depth-averaged value for each flume. In general, deposited beds in both flumes exhibited a series of steady states (characterized by constant final concentrations). Higher suspension concentrations were obtained with kaolinite than with mud at the same applied shear stress. At high shear stresses, particularly in the annular flume, plots appear to indicate a nearly linear increase of concentration with time (Figure 15). In these cases, either the samples were not collected for a sufficient time period to reach steady state concentrations, or the bed shear stress had exceeded the maximum bed shear strength (Parchure, 1984).

Placed Bed. Figures 17 through 20 are concentration-time profiles of placed beds. Again, the suspension concentration is a depth-averaged quantity. In general, the profiles are linear. The placed mud bed in the annular flume, Figure 19, exhibits an initial pattern of steady states at low shear stresses. This behavior occurred because it was difficult to add water to the flume initially without disturbing the bed; thus the top sediment layers behaved like deposited beds. Also observed in this figure is a sudden drop in the concentration at the beginning of the last three steps. It should be noted that the concentration plotted here is based on measurements at a single elevation approximately half way between the suspension surface and the bed. The concentration drop can be attributed to a change in the vertical concentration profile, rather than deposition, as a consequence of a change in the inter-particle collision frequency at the beginning of each step (Parchure, 1984). In the rocking flume, little erosion of the placed beds occurred before 0.3 N/m^2. In particular, the placed mud bed in the rocking flume Figure 20, did not start to erode until 0.4 N/m^2. Note that erosion occurred suddenly without any increase in applied shear stress. This type of behavior may be attributed to a decrease in the bed shear strength (bed softening) under the oscillatory velocity field in the rocking flume (Maa, 1986).

Bed Shear Strength

Deposited Bed. The final, steady state suspension concentration for each shear stress was first converted to mass per unit bed area and then plotted against the applied bed shear stress. Two linear plots of slopes M_1 and M_2 are obtained (see for example Fig. 21). By extrapolating the M_1 line back to the abscissa the bed surface shear strength τ_{so}, corresponding to initiation of erosion can be determined (Parchure and Mehta, 1985). Likewise the point of intersection of lines M_1 and M_2 gives the characteristic shear strength, τ_{sc}, above which the rate of erosion increases significantly. Bed surface (z=0) shear strength, τ_{so}, and characteristic shear strength, τ_{sc}, values are given in Table 2. Figures 21 and 22 are plots of suspended sediment mass per unit bed surface area versus applied shear stress from which the values given in Table 2 have been obtained. Both the rocking flume and the annular flume data are on the same plot. For the kaolinite beds, Figure 21, the same curves were obtained in both flumes. Values of τ_{so} and τ_{sc} in Table 2 suggest that the mud generally had a somewhat higher resistance to erosion than kaolinite.

Table 2. Bed Surface Shear Strength, τ_{so}, and Characteristic Shear Strength, τ_{sc}, of Deposited Beds in the Annular Flume and the Rocking Flume

	Kaolinite		Mud	
Apparatus	τ_{so} (N/m^2)	τ_{sc} (N/m^2)	τ_{so} (N/m^2)	τ_{sc} (N/m^2)
Annular Flume	0.08	0.25	0.18	0.40
Rocking Flume	0.08	0.25	0.03	0.20

Placed Bed. Table 3 contains values of bed shear strength (uniform over depth) for placed beds in each apparatus. Figures 23 and 24 are plots of suspended sediment mass eroded per unit bed surface area per unit time (i.e. rate of erosion) versus shear stress for placed kaolinite and mud beds, respectively. These plots were used to obtain values given in Table 3. The mud bed may be considered to have a somewhat higher shear strength than the kaolinite bed. However, contrary to the bed softening trend expected in the rocking flume, the shear strength was higher in this flume than in the annular flume. A possible explanation is noted later.

Table 3 Shear Strength of Placed Beds in the Annular Flume and the Rocking Flume

Apparatus	τ_s (N/m^2)	
	Kaolinite	Mud
Annular Flume	0.25	0.22
Rocking Flume	0.28	0.40

Relationship of Shear Strength to Depth

The density profiles coupled with concentration-time profiles presented earlier were used to produce profiles of the bed shear strength with depth. Details of procedure are given by Parchure and Mehta (1985).

Deposited Bed. Figures 25 and 26 are plots of bed shear strength versus depth. The same density profile for a given sediment was used for both flumes. The bed shear strength is observed to increase with depth below the bed surface. For the kaolinite bed, the profiles resulting from the two flumes are nearly coincident. For the mud bed, the profiles from the two flumes differ; the shear strengths from the rocking flume are lower. This difference is believed to be due to bed softening.

At corresponding depths in the bed, the shear strength of the mud is generally higher than that of kaolinite in the annular flume. In the rocking flume, shear strengths of kaolinite and mud at corresponding depths are nearly the same.

Placed Bed. The kaolinite bed yielded a constant depth versus shear strength profile, with a shear strength of 0.25-0.28 N/m^2, see Table 3, with only a small difference between the values obtained in the two apparatuses. Figure 27 is a plot of depth versus shear strength for the placed mud bed in the annular flume. Unlike the kaolinite beds, the profile is not constant, but has a lower shear strength in the top few millimeters, due to the deposited bed-like behavior noted previously. The shear strength of the placed mud bed in the rocking flume was 0.40 N/m^2, as estimated from Figure 24.

Erosion Rate

Deposited Bed. For a deposited bed under a constant shear stress the rate of erosion decreases with time. The relationship given by Eq. 1 describes the rate of erosion. The calculated rate coefficients α and ε_f are contained in Table 4 (Parchure and Mehta, 1985). Figures 28 and 29 are plots of the log of the erosion rate versus the square root of the applied shear stress minus the bed shear strength, i.e., square root of the excess shear stress.

Table 4. Values of α and ε_f for Deposited Beds

Apparatus	Kaolinite		Mud	
	α ($m/N^{1/2}$)	ε_f (mg/cm^2-hr)	α ($m/N^{1/2}$)	ε_f (mg/cm^2-hr)
Annular Flume	5.1	2.1×10^{-3}	7.9	3.2×10^{-3}
Rocking Flume	5.1	2.1×10^{-3}	7.9	2.0×10^{-3}

Placed Bed. For a placed bed the rate of erosion is given by Eq. 2. The values of M and τ_s are given in Table 5. Figures 23 and 24 are plots of erosion rate versus applied shear stress for kaolinite and mud, respectively. The erosion coefficient, M, was the same in both flumes for the kaolinite beds until the applied shear stress equalled 0.4 N/m^2 at which point the erosion rate increased rapidly in the rocking flume. However, there were insufficient data points to evaluate the coefficient M. The same situation occurred with

Table 5. Values of M and τ_s for Placed Beds

Apparatus	Kaolinite		Mud	
	M (mg/cm^2-hr)	τ_s (N/m^2)	M (mg/cm^2-hr)	τ_s (N/m^2)
Annular Flume	18.6	0.25	5.8	0.22
Rocking Flume	18.6	0.28	-	0.40

the mud bed in the rocking flume. It is noteworthy that in the rocking flume, the erosion rate increased suddenly in both cases (kaolinite and mud) in spite of the fact that the shear stress was constant at 0.4 N/m^2 (see Figs. 18 and 20). It is believed that bed softening under oscillatory current was a possible cause of this behavior.

IV. CONCLUDING REMARKS

A comparison of results obtained in both the annular flume and the rocking flume indicates trend similarities as well as quantitative differences in the erosional behavior of the two cohesive sediments.

Comparisons have been made of concentration-time profiles, shear strength variation with depth as a function of bed structure, and erosion rate. The concentration-time profiles for deposited beds were characterized by a series of steady states in both flumes and for both sediments. At high shear stresses (equal to or greater than 0.5 N/m^2), the concentration typically continued to increase linearly for the entire sampling period. The explanation for this behavior is the nature of the vertical distribution of shear strength. With increasing depth the shear strength increased, but at smaller rates until it was nearly constant. A one and a half hour sampling period was apparently insufficient to erode away the material to a depth at which the applied shear stress equalled the shear strength. Alternatively, the same type of behavior can be shown to result if the applied bed shear stress exceeds the maximum bed shear strength (Parchure and Mehta, 1985).

Placed beds exhibited a linear increase in suspension concentration with time. The initial period of testing may exhibit a pattern more like that of a deposited bed, as in Figure 19. The reason for this trend is that upon initial addition of water to the flume some disruption of the surface occurred even though care was taken in the addition of water. In general, the values obtained for suspension concentration from the placed beds were lower than for the deposited beds under the same flow conditions. Placed beds are typically more dense to begin with and are less erodible than deposited beds.

An important observation to note about placed beds in the annular flume is that after the applied shear stress was increased, the concentration of sediment in suspension actually decreased, in some instances. A similar

observation was made by Parchure (1984). There are two possible mechanisms involved in an interpretation of this phenomenon. The first is simply a delay in the response of the bed to an increase in the shear force being exerted on it. Secondly, increasing the rate of turbulent shearing in the water column increases the number of collisions between particles which enhances the rate of aggregation. Larger aggregates would be able to deposit, thereby reducing the suspension concentration.

The deposited mud bed had a lower bed shear strength (with respect to erosion) when subjected to an oscillatory current (in the rocking flume) as compared to a steady current (in the annular flume). The difference between shear strengths obtained with the two types of currents also increases with depth in the bed (see Figure 26). In general, the bed shear strength was lower under oscillatory currents than under steady currents. This feature is probably due to the bed softening under oscillatory currents, implying a degradation of bed shear strength due to a breakdown of the structure of the deposited aggregates. The coefficients α and ε_f of the erosion rate expression were comparable, however.

Placed beds in the rocking flume showed a sudden increase in the erosion rate without increasing the applied shear stress. The mud bed began to erode after about one hour at a shear stress of 0.4 N/m^2, while the erosion rate of kaolinite approximately doubled after about 45 minutes at the same shear stress (0.4 N/m^2). These sudden increases in erosion rate imply that at the time of occurrence of these changes, the bed shear strength decreases to a level below the applied shear stress.

The bed shear strength of placed beds was nearly the same for kaolinite in both flumes, but was higher for mud in the rocking flume than in the annular flume. This trend is seemingly in contradiction to the bed softening phenomenon noted. Maa (1986) however noted that under certain conditions depending upon the initial bed structure and flow conditions, a breakdown of aggregate structure within the bed is accompanied by an enhanced rate of consolidation. If the influence of consolidation on bed erodibility exceeds that due to structural breakdown, the bed would become more erosion resistant under oscillatory flows in comparison with steady flows.

The coefficient M of the erosion rate expression for kaolinite was the same under both types of currents. The results for mud could not be compared because there were insufficient data for mud from the rocking flume.

As noted, differences in the results between the two flumes may be the result of softening of the bed when subjected to an oscillatory current. The degree of softening is also dependent on the bed properties. The kaolinite bed was weaker than the mud bed, partly because it was less cohesive than the mud which contained montmorillonite as the predominant constituent. In a sense, kaolinite was already "softer" so it was not as readily affected by softening as mud.

The type of sediment used for an experiment had measurable influence on the results obtained. Kaolinite had a narrower distribution of (primary) particle size making a more homogeneous bed. The mud contained a sand fraction which does not erode by the same mechanism that fine particles do. The sand fraction can move as bedload or as suspended load, rather than as suspended load alone. Also, the mud contained an organic fraction which can sometimes lead to increased flocculation of particles.

In conclusion, higher bed shear strengths were generally obtained for mud than kaolinite, making the mud more resistant to erosion than kaolinite. Likewise, the erosion coefficient M for placed beds was 3 to 4 times larger for kaolinite as compared to mud. The type of current (steady or oscillatory) eroding the sediment appears to be an important factor in determining the erosion rate.

PART 2. SAN FRANCISCO BAY MUD

I. INTRODUCTION

Erosion tests conducted with mud from San Francisco Bay were for the purpose of evaluating the erosion potential of the mud at various bed densities. The test methodology, apparatus and procedure were the same as those of kaolinite and Cedar Key mud. Here therefore emphasis is placed predominantly on data analysis and interpretation.

II. SEDIMENT AND FLUID PROPERTIES

The predominant clay mineral constituent in the bay mud is montmorillonite, followed by illite, kaolinite, halloysite and chlorite. Among the non-clay minerals, quartz is predominant. There is also some iron (both structural, replacing some of the aluminum in illite, and non-structural, i.e., independent of the clay mineral) and organic matter. The cation exchange capacity of the samples used was 61 milliequivalents per hundred grams.

Suspended or recently deposited bay mud typically has a light brown color, while sediment from a depth of a few centimeters below the surface has a color ranging from light grey to black. When a sample of wet dredged sediment is placed in a glass cylinder and thoroughly stirred in water, a color change from dark grey to brown takes place. When allowed to stand, the color slowly changes back to greenish grey, and finally back to dark grey. These color changes occur due to the following reasons: in the dark grey sediment iron is present as ferrous sulfide. When stirred, ferrous sulfide is easily oxidized due to aeration to ferric hydroxide, which imparts a brownish color to the sediment. If allowed to stand, bacterial reduction first changes ferric iron to ferrous iron which is greenish, and then finally back to ferrous sulfide.

Table 6 gives sediment sample numbers and corresponding locations within the bay. In Table 7, sample properties - median size, bulk density, ρ_B, sediment density, ρ_s, and total organic matter are given. Sample 3A contained a sizeable fraction of sand; hence its median size (75 μm) was in the fine

sand range. This sample was therefore discarded from further analysis. The remaining samples were mixed in approximately equal proportions since they all had similar properties. Thus, erosion tests reported here are for the composited sample, a mixture of 1, 2A, 2B and 2C.

Table 6. Bay Mud Sample Locations

Sample No.	Location
1	Larkspur Channel
2A	Richmond Longwharf Manuevering Area
2B	Richmond Longwharf Manuevering Area
2C	Richmond Longwharf Manuevering Area
3A	Southampton Shoal Channel

Table 7. Bay Mud Sample Properties

Sample No.	Median size (μm)	Bulk density, ρ_B (g/cm^3)	Sediment density, ρ_s (g/cm^3)	Total organics (%)
1	3	1.52	2.76	10.0
2A	7	1.56	2.67	7.6
2B	30	1.69	2.76	3.4
2C	12	1.65	2.72	4.7
3A	75	1.90	3.11	2.2

The (eroding) fluid was tap water to which sodium chloride was added to raise the salinity to 33 ppt. The pH was maintained at ~ 9. The mean fluid temperature was 24°C during the experiments.

In tests with deposited beds, the pore fluid composition may be considered to have been the same as the eroding fluid composition given above. In the single test with a placed bed at natural density, the pore fluid composition was as follows: Na^{++} 9,700 ppm, Ca^{++} 940 ppm, Mg^{++} 1,150 ppm, K^{+} 770 ppm, Cl^{-} 16,930 ppm and SO_4^{--} 2,640 ppm. Solution conductivity was 33 mmhos/cm.

III. TEST RESULTS

Test conditions are summarized in Table 8. Test 1 was with a placed (dense) bed in the annular flume at the natural bulk density of 1.63 g/cm^3 (corresponding to a dry density of 0.96 g/cm^3). Tests 2 through 5 were for deposited (soft) beds with consolidation periods of 0.5 day and 3.8 days.

Table 8. Bay Mud Test Conditions

Test No.	Apparatus	Consolidation (days)	ρ_D (g/cm^3)	ρ_B (g/cm^3)
1	Annular flume	dense bed	0.96	1.63
2	Annular flume	0.5	0.22	1.17
3	Rocking flume	0.5	0.22	1.17
4	Annular flume	3.8	0.40	1.28
5	Rocking flume	3.8	0.40	1.28
P1	Straight flume[a]	40 (placed)	0.61[b]	1.36
P2	Straight flume[a]	15 (placed)	0.57[b]	1.34

[a]Tests of Partheniades (1965).

[b]Sediment density was 2.24 g/cm^3

Density profiles for the dense bed (test 1) and soft beds (tests 2,3,4,5) are given in Fig. 30. These are dry densities, ρ_D (not to be confused with sediment density, ρ_s). The dense bed density did not vary with depth. For the soft beds, ρ_D and ρ_B values given in Table 8 are representative depth-mean values corresponding to the top bed layers which eroded during the tests. Thus they are not averages over the entire mud bed thickness shown in Fig. 30.

Tests P1 and P2 corresponding to series I and II of Partheniades (1965) were conducted on remolded, placed beds. Since Partheniades also used sediment from the San Francisco Bay which is spatially well mixed (Krone, 1978), results from these tests are included in the subsequent analysis.

Time-concentration data for tests 1 through 5 are given in Figs. 31 through 35. Data from P1 and P2 appear elsewhere (Partheniades, 1962).

The erosion rate, ε, against bed shear stress, τ_b, relationship from test 1 (annular flume) is compared with P1 (series I) and P2 (series II) in

Fig. 36. The annular flume data agree with series I up to $\tau_b \simeq 0.8$ N/m^2. Disparities for larger τ_b are attributed to likely corresponding differences in the bed structure due to differences in the method of bed preparation, i.e., the manner in which the beds were remolded and placed. In series II, iron oxide from rust in the return pipe of the flume used by Partheniades enhanced bed resistance to erosion due to cementing of aggregates. Characteristically however, incipient erosion is observed to have begun at the same $\tau_b = \tau_{co}$, ~ 0.1 N/m^2, in all three cases.

In Fig. 37, erosion rate, ε, is plotted against τ_b for tests 1 through 5, i.e. for dense as well as soft beds, for the mere purpose of demonstrating similarities and differences. For the dense bed, time-concentration profiles (Fig. 31) were characteristically linear, hence ε was constant for a given τ_b. On the other hand, time-concentration response of the soft beds (Figs. 32, 33, 34, 35) was a series of steady state steps also characteristic of such beds. For all tests, ε was calculated for each τ_b by substracting the initial concentration from final concentration for each particular step and dividing the difference by the step duration (90 minutes). Thus, the ε value is a representative mean for the entire step. The most significant feature of Fig. 37 is the considerably higher resistance to erosion offered by the dense bed compared to the soft beds. In tests with soft beds, the bed softening role of oscillatory flow in the rocking flume is also evident, particularly in the 0.5 day consolidation test, when compared with the corresponding results from the annular flume.

The following analysis is directed towards determining the erosion rate constants, M and τ_c (= τ_s) of Eq. 2, from all the tests. τ_c is then correlated empirically to the bulk density and, finally, M is likewise correlated to τ_c. Equation 2 is an acceptable approximation for the erosion behavior of dense beds. For soft beds, Eq. 1 is applicable (Parchure and Mehta, 1985). However, Eq. 2 is a reasonable approximation of the erosion behavior of soft beds, provided the erosion rate is calculated as a representative mean of each steady state step as noted (Fig. 37).

In Figs. 38 and 39, ε-τ_b relationships for soft beds have been replotted for clarity. With reference to Fig. 39 as an example, τ_{co} is the value of τ_b corresponding to incipient erosion, while τ_c is the "operational" or "design" value of the critical shear stress for erosion applicable to Eq. 2. M is

evaluated from the slope of the second line. In Fig. 38, erosion rates at τ_b = 0.1 N/m^2 appear to be excessively high in comparison with the trends implied by other data from both flumes. These values, corresponding to points A and B, suggest mass erosion as opposed to surface erosion behavior (Parchure and Mehta, 1985). Therefore, points A and B were disregarded.

For the dense bed as well as tests of Partheniades, linear approximations (dashed lines) shown in Fig. 36 were used to evaluate τ_c and M. For the soft beds, Parchure (1984) used an alternative procedure for estimating τ_c. This involves plotting the final suspension concentration in a steady state step against the corresponding τ_b. This is done in Figs. 40 and 41 where C_{90} is the (final) concentration at 90 minutes, the step duration.

Results are summarized in Table 9. Characteristically, τ_{co} values are close to each other with a mean of 0.12 N/m^2. For the same sediment, incipient erosion occurs at the same shear stress because the surface shear strength (equal to applied shear stress) is unaffected by overburden. Hence bed preparation procedure or density do not significantly influence τ_{co}. τ_c has been calculated by two methods - A corresponding to Figs. 38, 39 and B corresponding to Figs. 40 and 41; the latter method being applied to deposited (soft) beds only, since for dense beds the two methods yield identical results. Values obtained by B are generally slightly lower (except in test 4) than A, but are of comparable magnitudes. M values are obtained from linear slopes in Figs. 36, 38 and 39.

In Fig. 42, τ_c (both methods) is plotted against ρ_B. The following may be considered as a representative relationship encompassing all data:

$$\tau_c = 1.04\ (\rho_B - 1) \tag{3}$$

In Fig. 43, M is plotted against τ_c yielding the following relationship (without consideration for the influences of bed structure or flow):

$$M = 1.06 \times 10^{-3} e^{-2.33\ \tau_c} \tag{4}$$

With respect to Eq. 3, the trend of increasing τ_c with bed density is in agreement with previous observations (Mehta et al., 1982). Likewise, others have previously reported the trend of decreasing M with increasing τ_c evident in Fig. 43 and Eq. 4 (Ariathurai and Arulanandan, 1978; Hunt, 1981).

Table 9. Bay Mud Erosion Rate Constants

Test No.	τ_{co} (N/m^2)	τ_c		M (g/cm^2-min)
		A (N/m^2)	B (N/m^2)	
1	0.12	0.65	-[b]	2.8×10^{-4}
2	0.16	0.35	0.23	3.2×10^{-4}
3	-[a]	0.12	0.05	5.0×10^{-4}
4	0.10	0.28	0.30	7.4×10^{-4}
5	0.10	0.28	0.20	7.4×10^{-4}
P1	0.12	0.38	-[b]	2.1×10^{-5}
P2	0.12	1.20	-[b]	7.8×10^{-5}

[a]Insufficient data

[b]Method A not applied

IV. CONCLUDING REMARKS

The relationships considered to be representative of the rate of erosion of bay mud are as follows:

$$\varepsilon = M \left(\frac{\tau_b}{\tau_c} - 1\right) \tag{2}$$

$$\tau_c = 1.04 \ (\rho_B - 1) \tag{3}$$

$$M = 0.00106 \exp(- 2.33 \ \tau_c) \tag{4}$$

$$\tau_b = \frac{\rho g n^2}{h^{1/3}} u^2 \tag{5}$$

noting that in Eq. 2, τ_c and τ_s, used previously, have the same meaning.

In Eq. 5, n is Manning's bottom resistance coefficient, h is depth of flow and u is current speed. An example is considered in Fig. 44 where the rate of erosion, ε, is plotted against current speed, u, (0-1.5 m/sec), for different values of the bed bulk density, ρ_B (1.2, 1.4 and 1.6 g/cm^3). h = 10 m and n = 0.020 were selected arbitrarily as typical representative estuarine values. The influence of ρ_B (which also reflects bed "aging") on ε

in this "design chart" is observed to be quite significant. Soft beds (1.2 g/cm^3) generally have an order of magnitude ($\sim 10^{-2}$ g/cm^2-min) greater rate of erosion than do dense (1.6 g/cm^3) beds ($\sim 10^{-3}$ g/cm^2-min) at the same speed ($\sim$ 1.3 m/sec).

APPENDIX

VELOCITY AND SHEAR STRESS CALCULATIONS

The original plan for the rocking flume designated a height of 22 cm. Early experiments determined that this height would not allow for sufficient water depth to generate a large enough shear stress on the bed surface. The height of the flume was therefore increased to 36 cm. A second modification was made with the addition of a plexiglass top constriction over the center of the flume (Fig. 6b,c). This constriction increased the flow velocity over the sediment bed. The top could be set at any selected depth over the bed.

Flume Calibration. To calculate the shear stress in the flume it was necessary to know the velocity of water above the bed. Three different techniques were used to measure velocity. In all cases maximum velocity was measured. Following is a brief description of the methods employed and a comparison of the results obtained. Calculations are made of the shear stress with and without the top in place. Calibration marks were added to the speed controller of the flume, so that wave period and velocity could be determined at specific settings.

For a shallow water wave the velocity profile over the water depth is fairly constant, at least within the detection limits employed. The simplest method of measuring velocity is to determine the horizontal displacement of a particle floating on the surface at the node. From the distance traveled the maximum velocity can be calculated from the relationship $u_m=\pi d/T$ where d is displacement and T is wave period. This measurement could only be made without the top constriction in the flume. Once the top was in place new estimates of velocity were made by assuming that the only effect of the top was to increase water velocity at the center of the flume. From the equation of continuity, the same volume of water, 17.5 cm deep, had to pass the center, but there were only 10 cm of depth for it below the top. New velocities were calculated from a ratio of water depths at the ends and the middle of the flume. A ratio of 1.75 (velocity with top divided by velocity without top) was determined. Table A.1 contains velocities obtained by the method of horizontal displacement.

Table A.1. Maximum Velocities Obtained by Measurement of Horizontal Displacement, without and with Top Constriction

Wave period, T (sec)	Horizontal displacement, d (cm)	Maximum velocity, u_m without top (cm/sec)	Maximum velocity, u_m with top (cm/sec)
13.0	25	6.0	10.6
8.0	27	10.6	18.6
6.6	28	13.3	23.3
6.1	30	15.5	27.0
5.7	33	18.2	31.8
5.4	36	20.8	36.4
5.2	38	23.0	40.2
5.1	40	24.6	43.1
5.0	50	31.7	55.5

The most direct method of measuring velocity was with a current meter. The current meter was an electro-magnetic unit made by Marsh McBirney (model 523), with an accuracy of 3 cm/s. Measurements were taken at a height of 2 cm above the bed at the center of the flume. Data were recorded on a Hewlett-Packard strip chart recorder so that the mean maximum velocity could be determined. Table A.2 contains velocity (and wave period) data obtained using the meter.

The third method involved measuring the displacement of water above and below still water level, at the ends of the flume. Velocity was calculated by determining the total volume of water that moved through the flume without and with the top in place over one-half a wave period (see Fig. A.1). The maximum velocity, u_m, without the top is

$$u_m = \frac{\pi A_d}{hT} \tag{A.1}$$

where A_d is the longitudinal (vertical) area of water displaced during one-half period, and h is the still water depth. A_d is obtained from (for small displacements):

Table A.2. Periods of Oscillation and Velocities Obtained from Current Meter in the Rocking Flume

Period, T (sec)	Max.velocity, u_m (cm/sec)
33.6	3.1
35.0	3.7
21.5	4.6
13.0	10.5
11.0	13.7
9.1	16.3
7.8	19.1
7.4	20.1
7.2	20.8
6.6	23.4
6.1	27.0
5.7	32.3
5.5	36.4
5.2	43.0
5.1	47.0

Table A.3. Maximum Velocities Obtained by Considering Flow Continuity

Wave period, T (sec)	Maximum velocity, u_m without top (cm/sec)	Maximum velocity, u_m with top (cm/sec)
13.0	4.8	8.1
8.0	9.2	15.4
6.6	12.0	20.7
6.1	14.3	26.0
5.7	15.9	32.1
5.5	19.5	36.2
5.2	20.7	45.0
5.1	23.8	52.0

$$A_d = L \left(\frac{A}{\pi} + \frac{B}{4}\right) \qquad (A.2)$$

where A/2 = vertical displacement amplitude at flume ends relative to still water level, B/2 = vertical displacement amplitude of flume bottom and L = flume length. In Eq. A.2, the water surface profile is assumed to vary sinusoidally. With the top in place, A_d was appropriately modified. Results are presented in Table A.3.

The maximum applied shear stress was calculated from the following relationships established by Jonsson (1966); $\tau_{max}=0.5\rho f_w u_m^2$, where ρ is water density, f_w is the coefficient of friction, and u_m is maximum velocity. The coefficient of friction can be calculated as $f_w=0.09\ Re^{-0.2}$, where Re is the wave Reynolds number. The Reynolds number can be calculated as $u_m^2/\sigma\nu$, where u_m is maximum velocity, σ is wave angular frequency ($2\pi/T$), and ν is kinematic viscosity of water. For these experiments the kinematic viscosity was taken to be 1×10^{-2} cm^2/sec and ρ as 1 g/cm^3. These calculations are based on fresh water.

Calculation of shear stress using Jonsson's formula yields the maximum applied shear stress. This formula is valid for progressive waves generating (smooth) turbulent flows. In dealing with a standing wave, the applied shear stress is not constant, but oscillates as a square sine function. To adjust for this difference the maximum velocity was used to calculate a maximum shear stress, τ_m. By integrating shear stress over one-half a wave period the mean shear stress was determined. The result is that mean shear stress is one-half the maximum shear stress. Justification for this manipulation was based on the correlation of results of critical shear stresses obtained in the rocking flume compared to those obtained in the annular flume.

A calibration curve between maximum velocity, u_m, and wave period, T, is presented in Fig. A.2, based on data in Tables A.1, A.2 and A.3. The corresponding relationship between the average bed shear stress, τ_b, and wave period, T, is given in Fig. A.3.

LITERATURE CITED

American Public Health Association, Standard Methods for the Examination of Water and Wastewater, 14th ed., American Public Health Association, New York, 1975.

Ariathurai, R., and Arulanandan, K., "Erosion of Cohesive Soils," Journal of the Hydraulics Division, ASCE, Vol. 104, No. HY2, February, 1978, pp. 279-283.

ASTM, 1981 Annual Book of ASTM Standards, American Society for Testing and Materials, Philadelphia, Pennsylvania, 1981.

Hunt, S.D. and Mehta, A.J., "An Evaluation of Laboratory Data on Erosion of Fine Sediment Beds," Paper Presented at the Annual Meeting of the Fine Particle Society, Miami, Florida, April, 1985.

Jonsson, I.G., "Wave Boundary Layers and Friction Factors," Proceedings of the 10th Coastal Engineering Conference, ASCE, Vol. 1, Tokyo, Japan, 1966, pp. 127-148.

Krone, R.B., "Sedimentation in San Francisco Bay System," In: San Francisco Bay: The Urbanized Estuary, California Academy of Sciences, San Fancisco, California, 1979, pp. 177-190.

Maa, P.Y., "Erosion of Soft Muds by Waves," Ph.D. Dissertation, University of Florida, Gainesville, Florida, 1986.

Mehta, A.J., "Depositional Behavior of Cohesive Sediments," Ph.D. Dissertation, University of Florida, Gainesville Florida, 1973.

Mehta, A.J., Parchure, T.M., Dixit, J.G., and Ariathurai, R., "Resuspension of Deposited Cohesive Sediment Beds," In: Estuarine Comparisons, V.S. Kennedy Editor, Academic Press, New York, 1982, pp. 591-609.

Parchure, T.M., "Erosional Behavior of Deposited Cohesive Sediments," Ph.D. Dissertation, University of Florida, Gainesville, Florida, 1984.

Parchure, T.M. and Mehta, A.J., "Erosion of Soft Cohesive Sediment Deposits," Journal of Hydraulic Engineering, ASCE, Vol. 3, No. 10, October 1985, pp. 1308-1326.

Partheniades, E., "A Study of Erosion and Deposition of Cohesive Soils in Salt Water," Ph.D. Dissertation, University of California, Berkeley, California, 1962.

Partheniades, E., "Erosion and Deposition of Cohesive Soils, Journal of the Hydraulics Division, ASCE, Vol. 91, No. HY1, January, 1965, pp. 105-139.

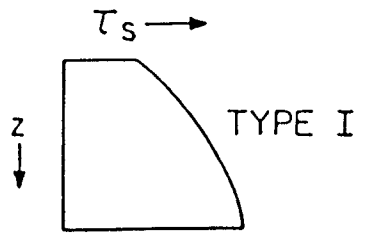

Fig. 1. Variation of Bed Shear Strength with Depth for a Deposited Bed, Type I Profile (after Parchure, 1984).

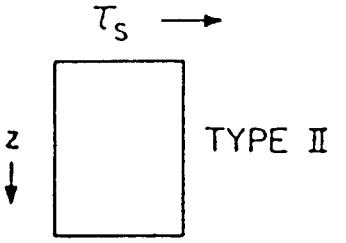

Fig. 2. Variation of Bed Shear Strength with Depth for a Placed Bed, Type II Profile (after Parchure, 1984).

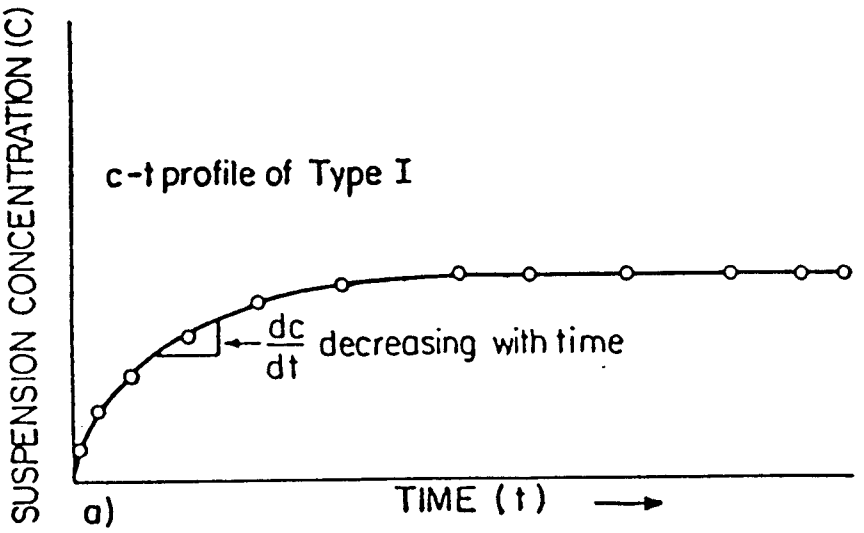

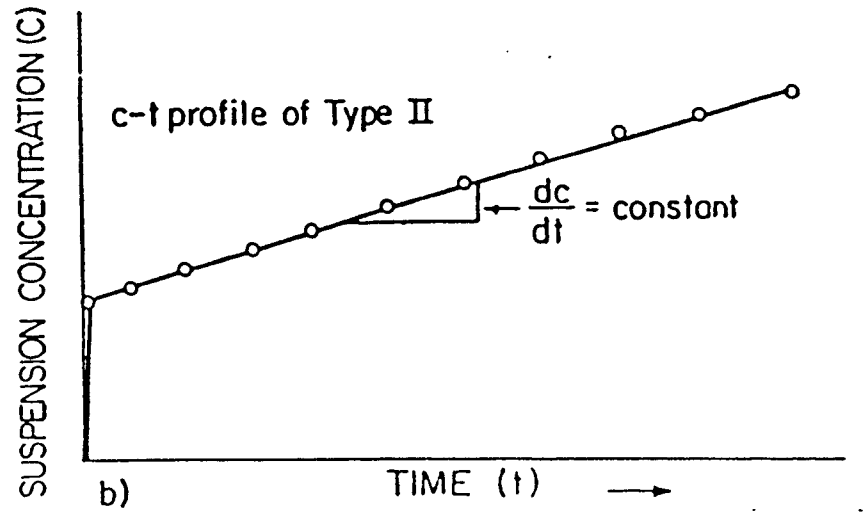

Fig. 3a. Concentration-Time Profile for a Deposited Bed (Type I) (after Parchure, 1984).

Fig. 3b. Concentration-Time Profile for a Placed Bed (Type II) (after Parchure, 1984).

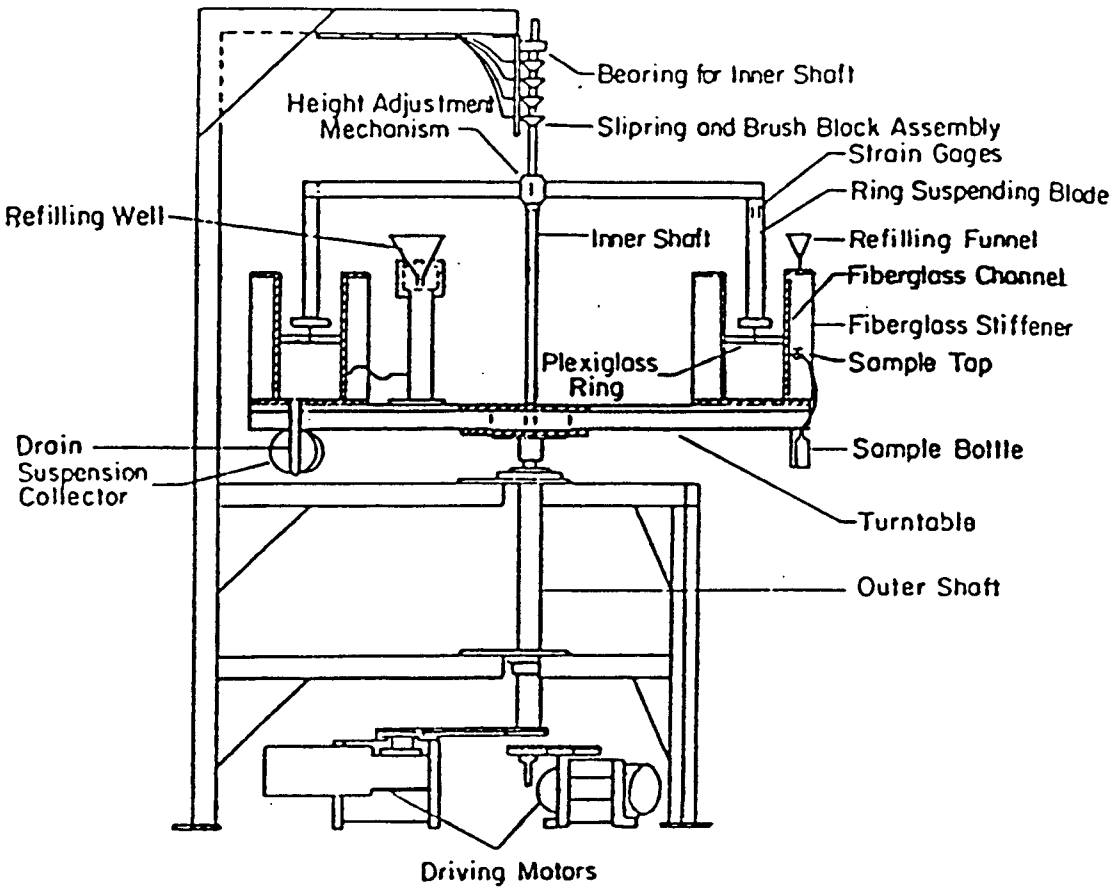

Fig. 4. Schematic View of Annular Flume (after Mehta, 1973).

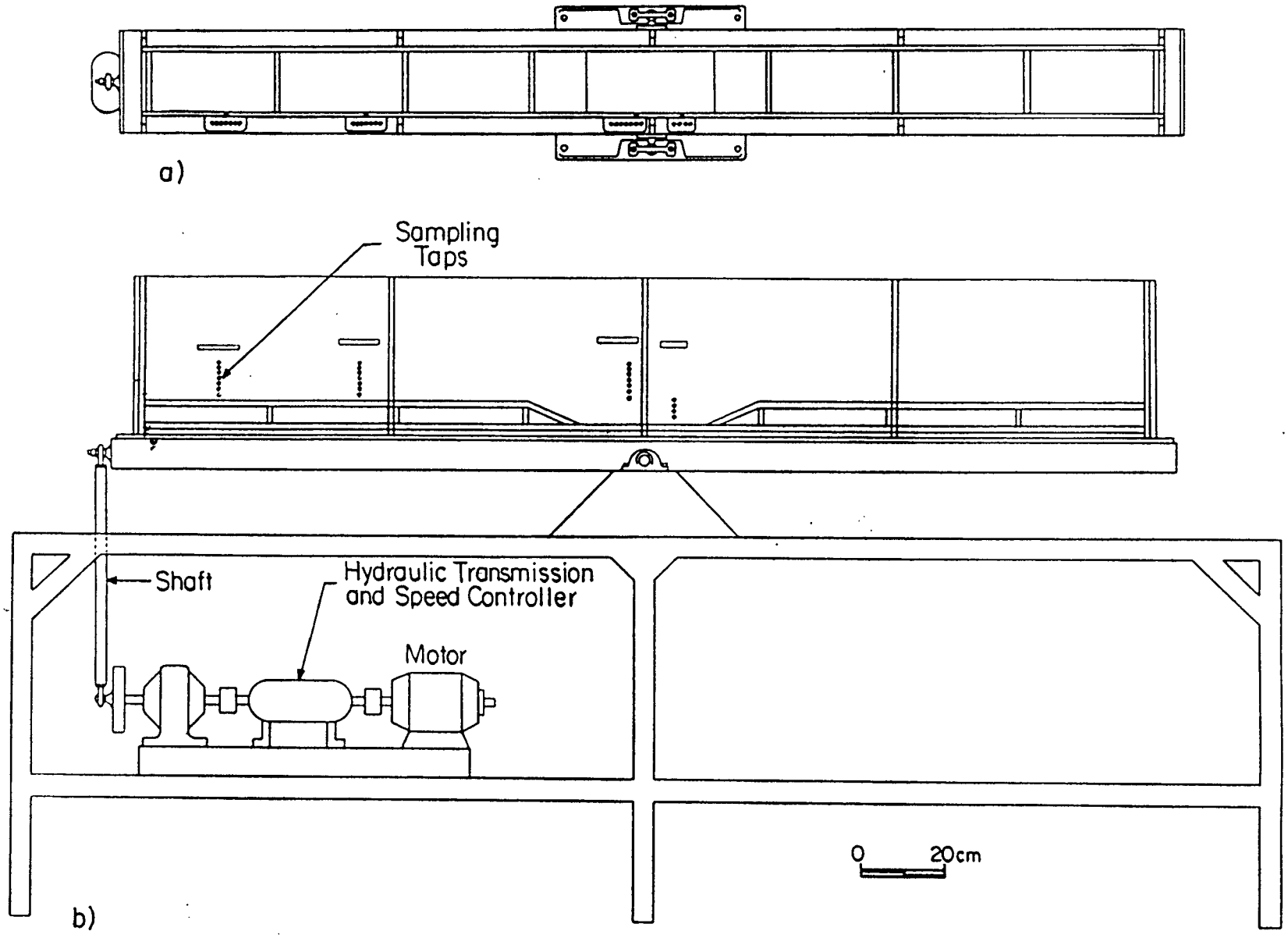

Fig. 5a. Plan View of Rocking Flume.
Fig. 5b. Elevation View of Rocking Flume.

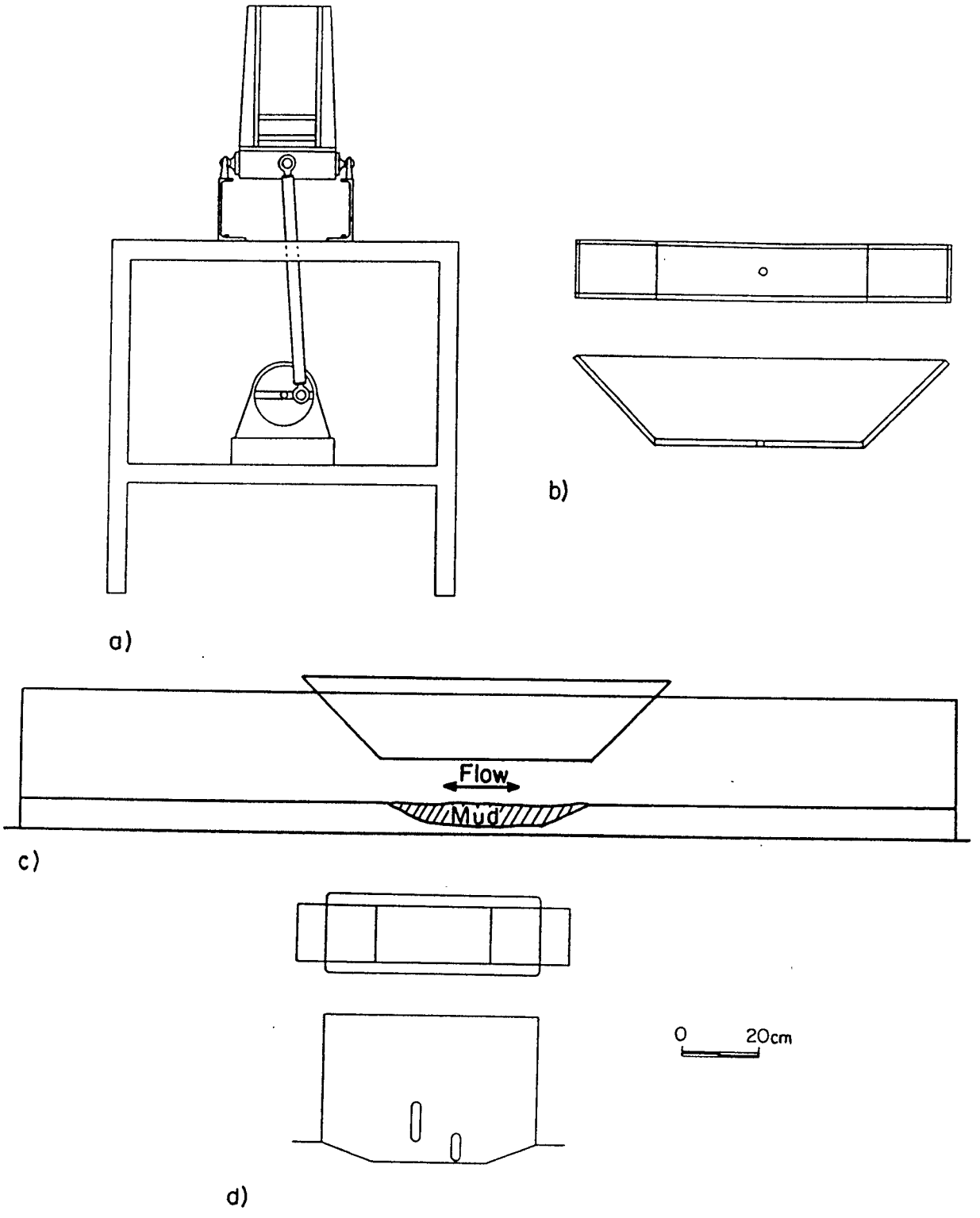

Fig. 6a. Side View of Rocking Flume.
Fig. 6b. Top Constriction for Rocking Flume.
Fig. 6c. Top Constriction Placed in the Rocking Flume.
Fig. 6d. Removable Sheet Metal Bed for Rocking Flume.

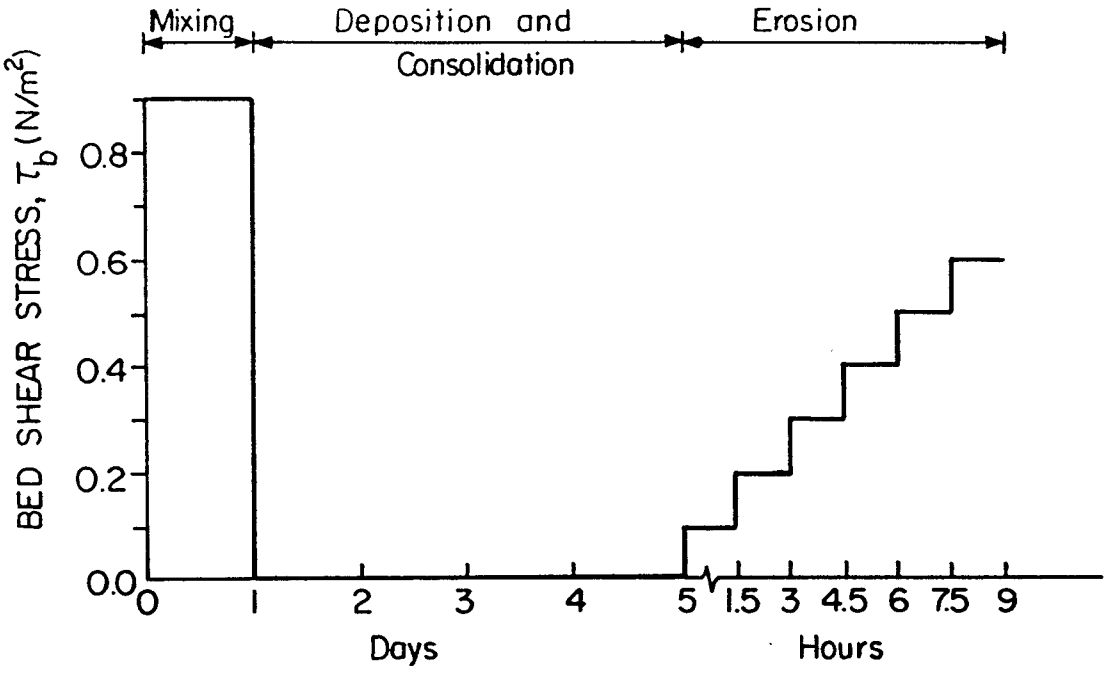

Fig. 7. Experimental Test Procedure (Shear Stress Variation).

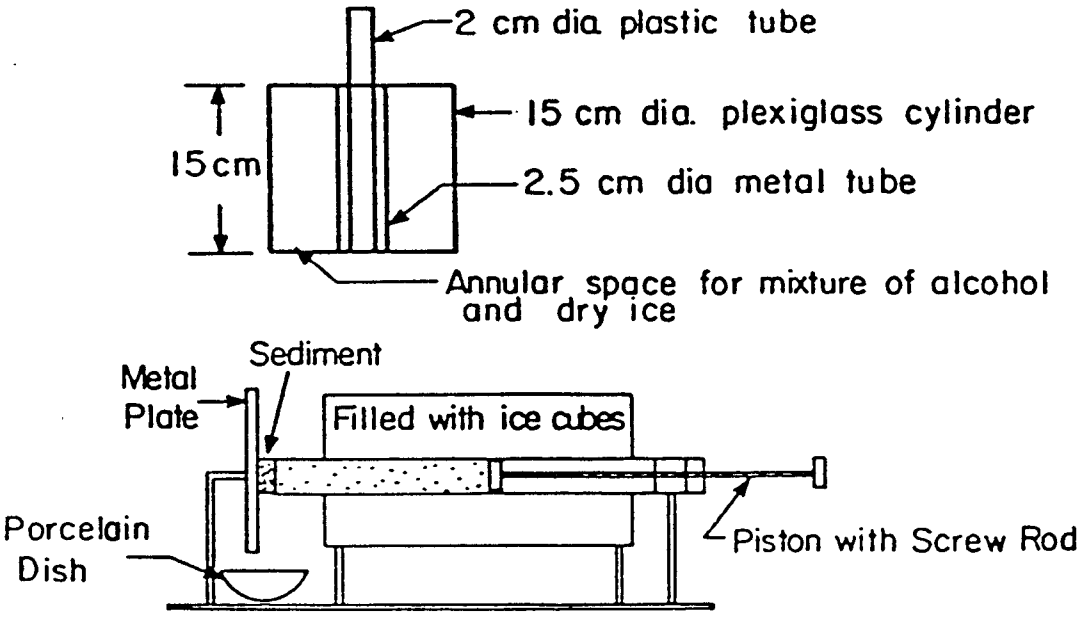

Fig. 8. Apparatus for Measurement of Density as a Function of Depth (after Parchure, 1984).

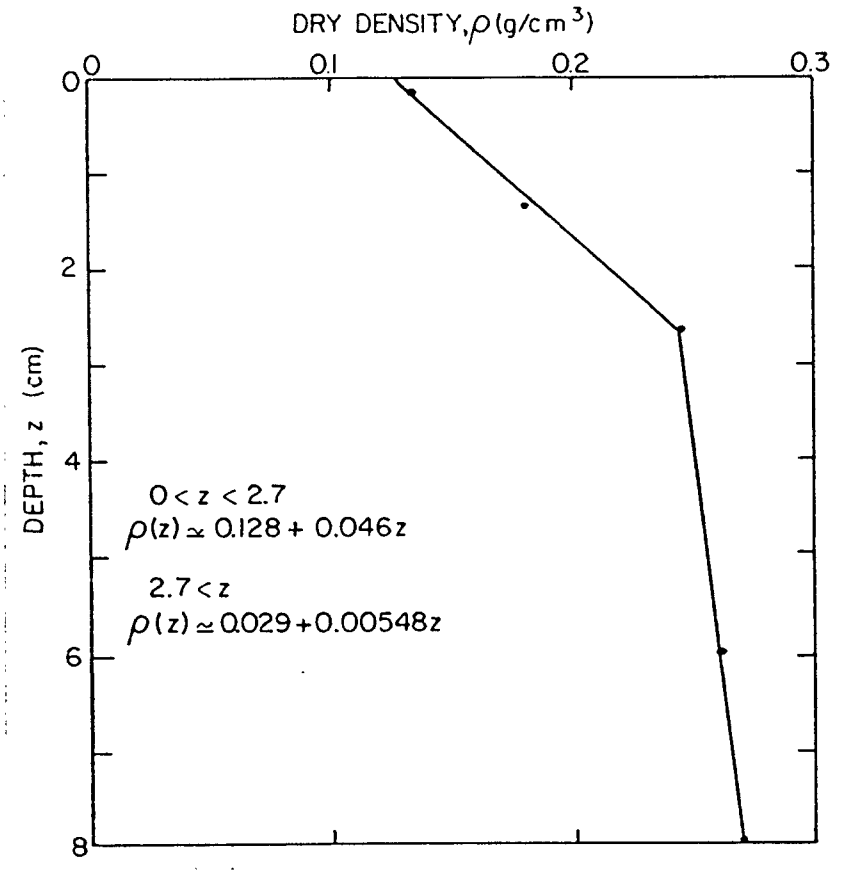

Fig. 9. Density (Dry) Profile as a Function of Depth for Deposited Kaolinite.

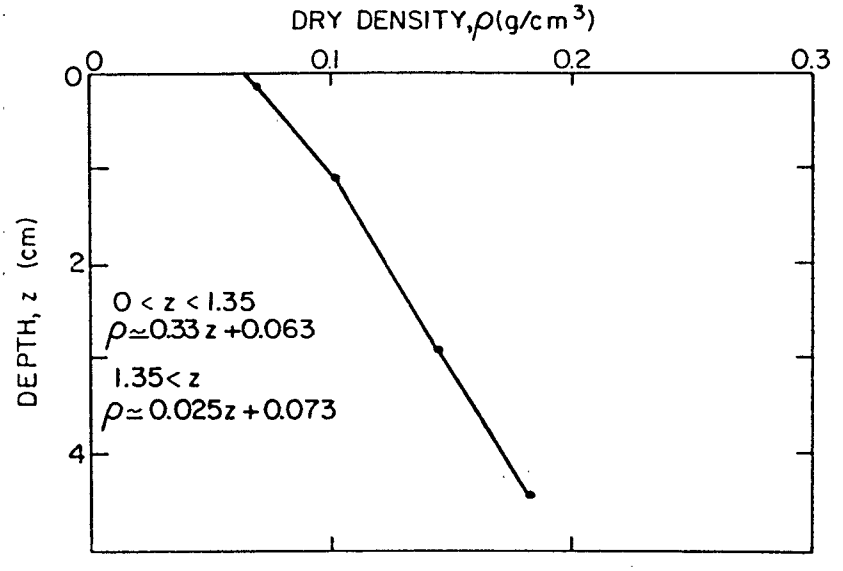

Fig. 10. Density (Dry) Profile as a Function of Depth for Deposited Cedar Key Mud.

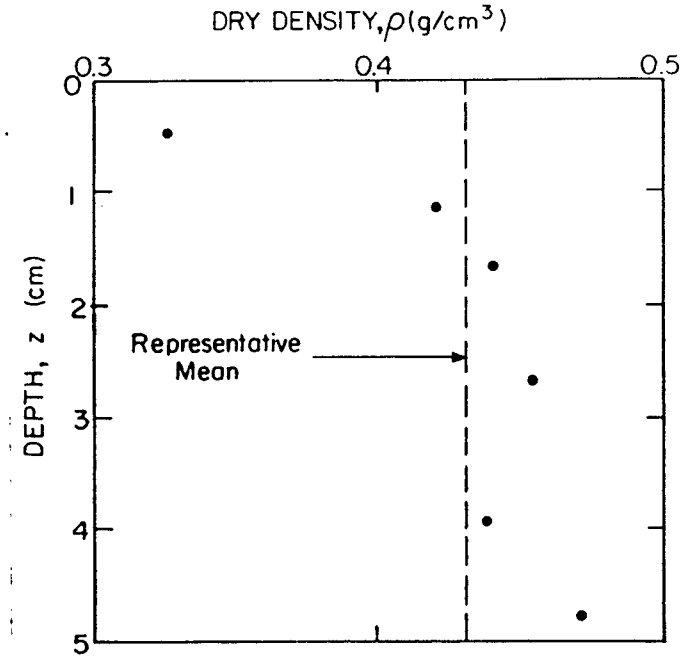

Fig. 11. Density (Dry) Profile as a Function of Depth for Placed Kaolinite.

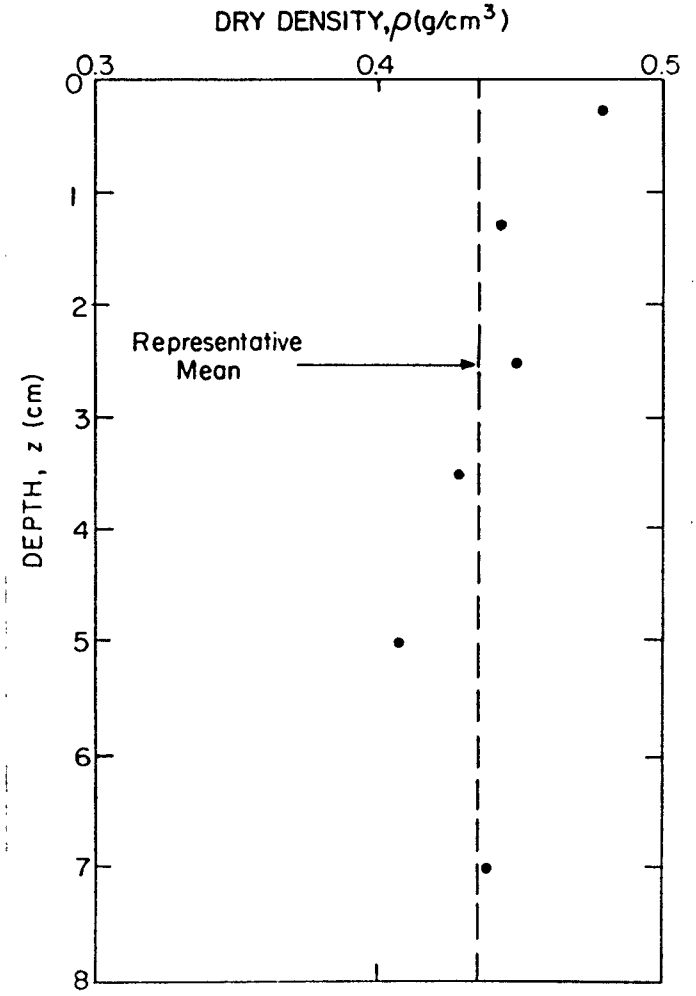

Fig. 12. Density (Dry) Profile as a Function of Depth for Placed Cedar Key Mud.

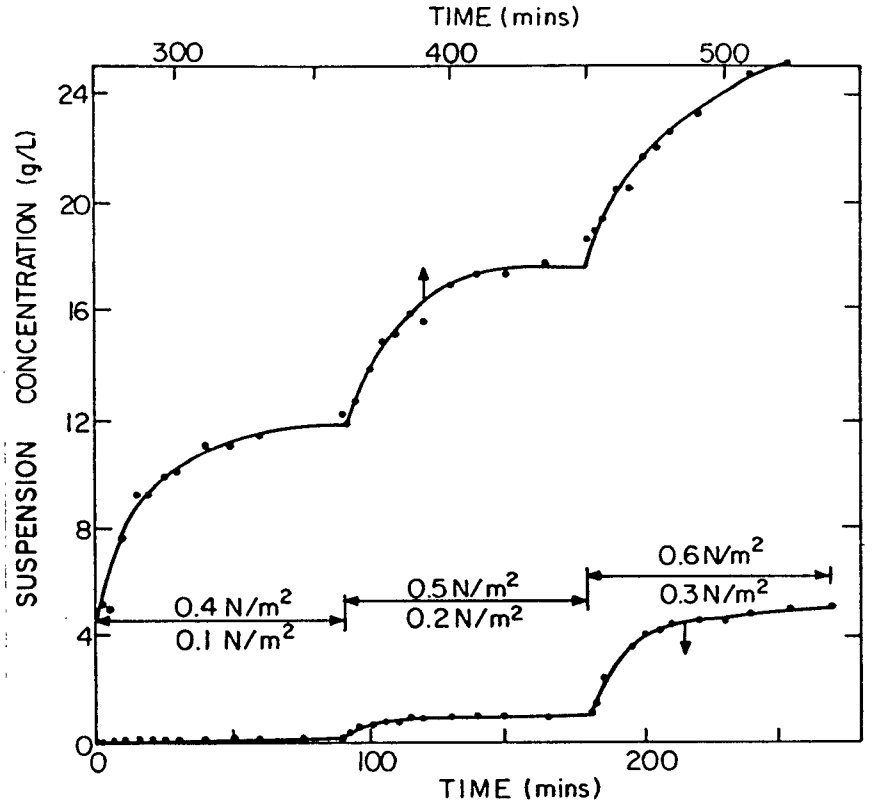

Fig. 13. Suspended Sediment Concentration versus Time for Deposited Kaolinite, Annular Flume.

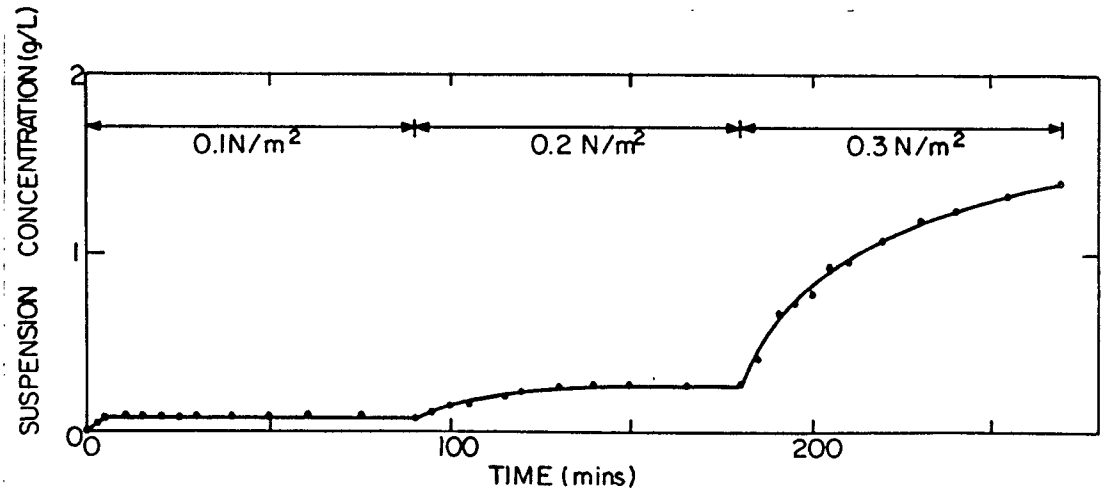

Fig. 14. Suspended Sediment Concentration versus Time, Deposited Kaolinite, Rocking Flume.

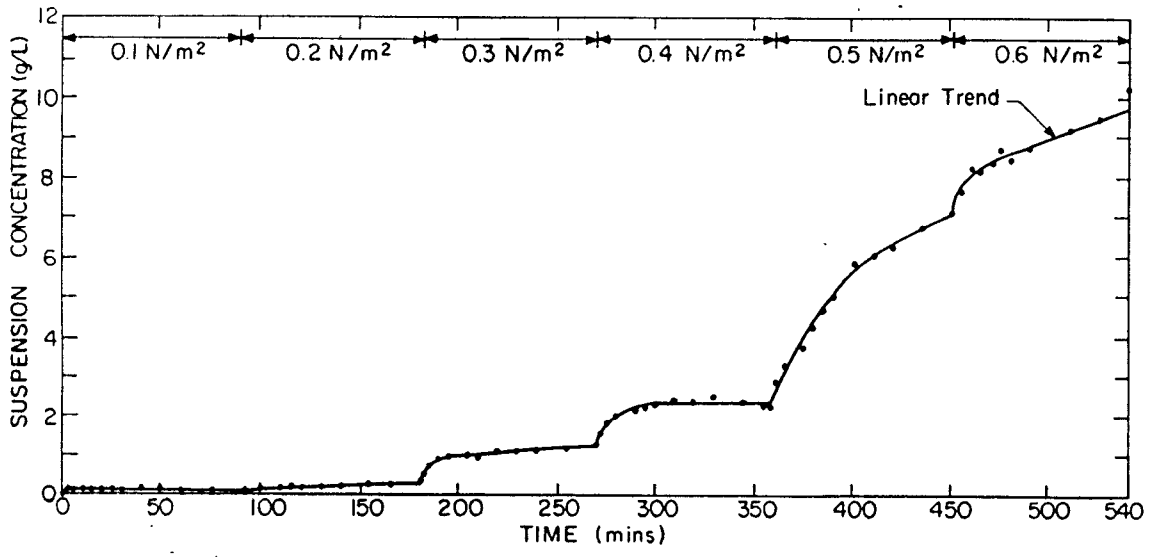

Fig. 15. Suspended Sediment Concentration versus Time for Deposited Cedar Key Mud, Annular Flume.

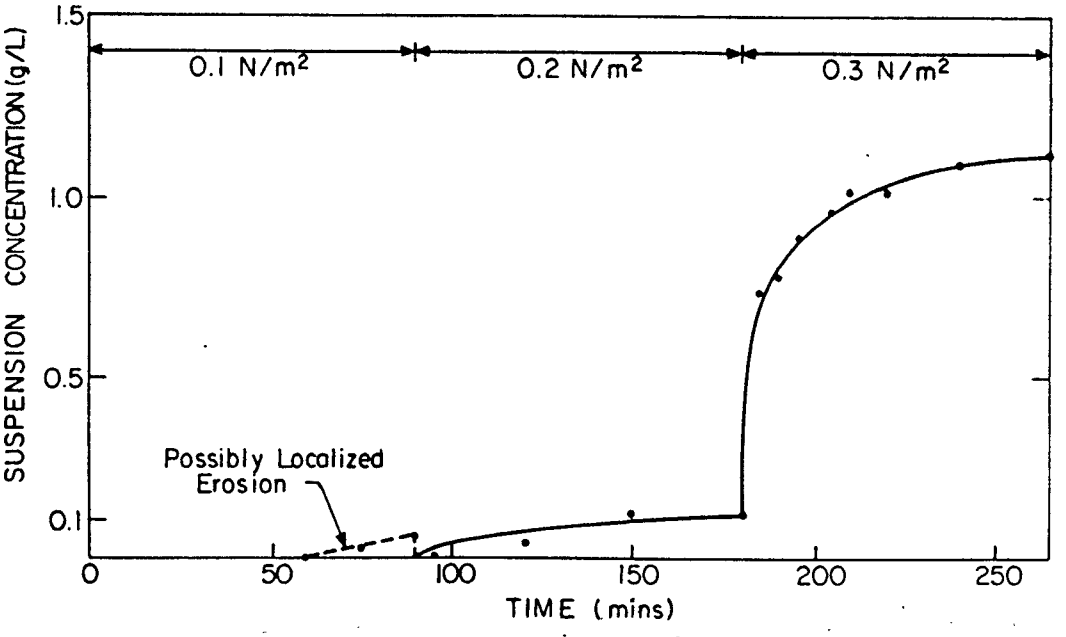

Fig. 16. Suspended Sediment Concentration versus Time, Deposited Cedar Key Mud, Rocking Flume.

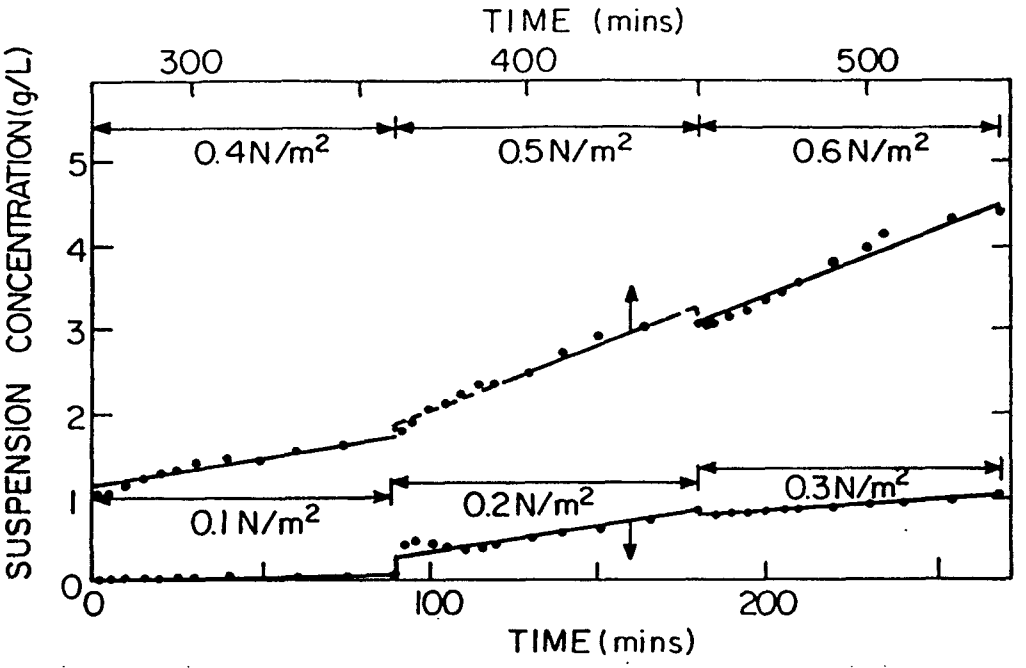

Fig. 17. Suspended Sediment Concentration versus Time, Placed Kaolinite, Annular Flume.

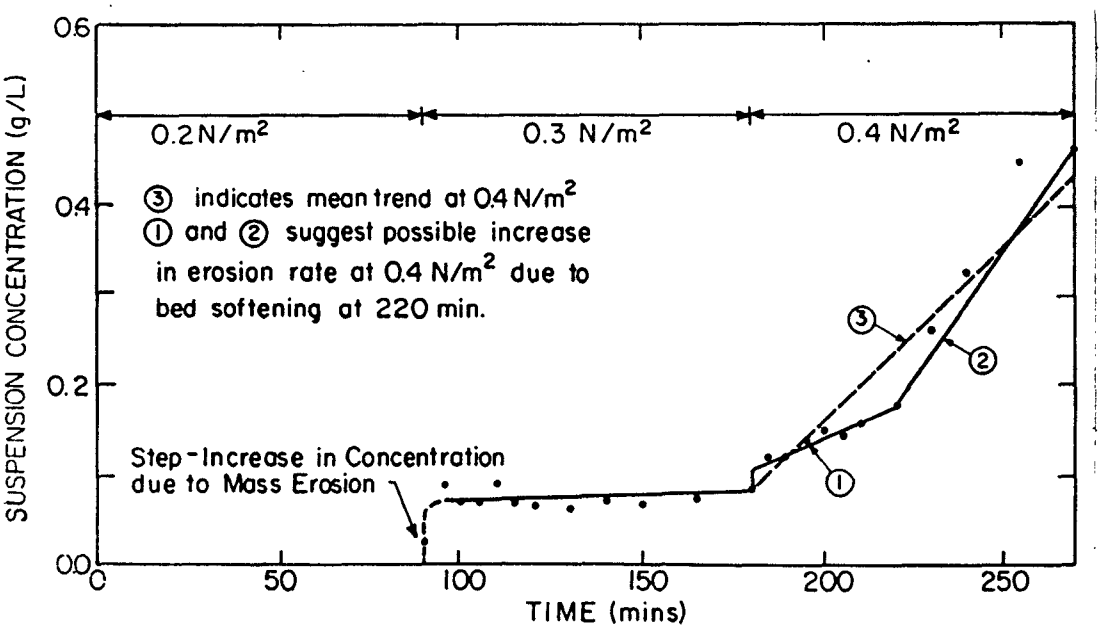

Fig. 18. Suspended Sediment Concentration versus Time, Placed Kaolinite, Rocking Flume.

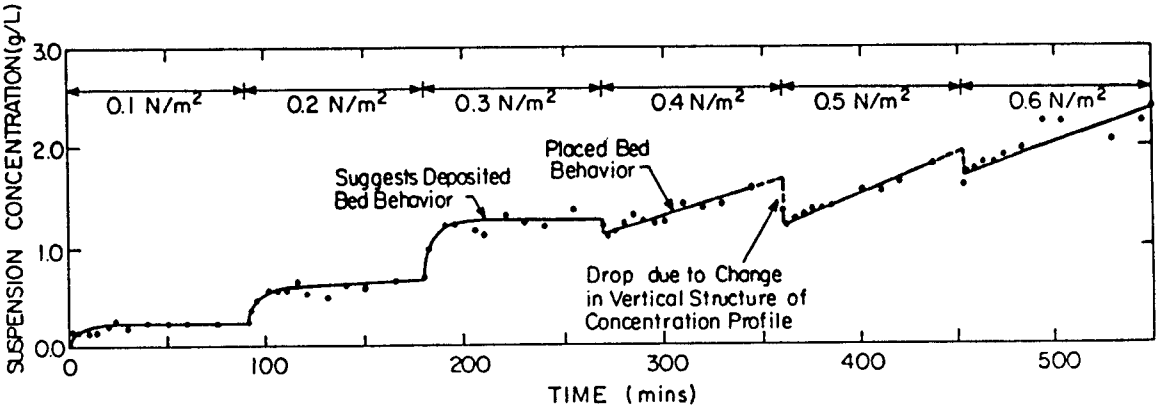

Fig. 19. Suspended Sediment Concentration versus Time, Deposited Cedar Key Mud, Annular Flume.

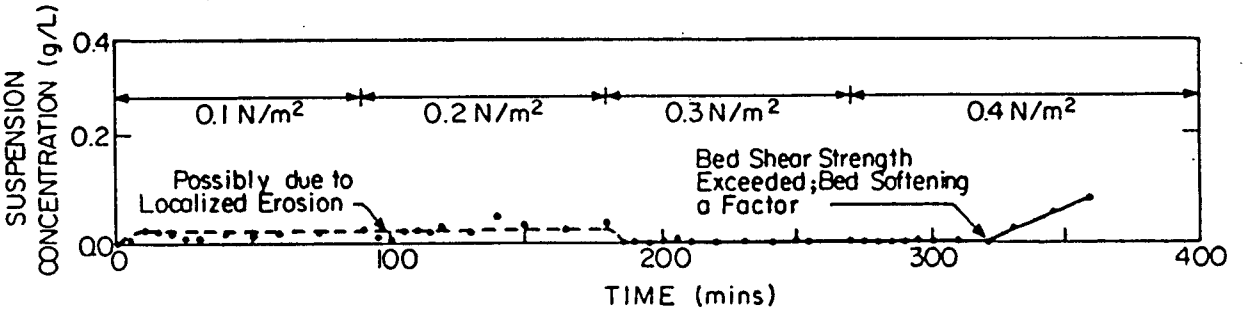

Fig. 20. Suspended Sediment Concentration versus Time, Placed Cedar Key Mud, Rocking Flume.

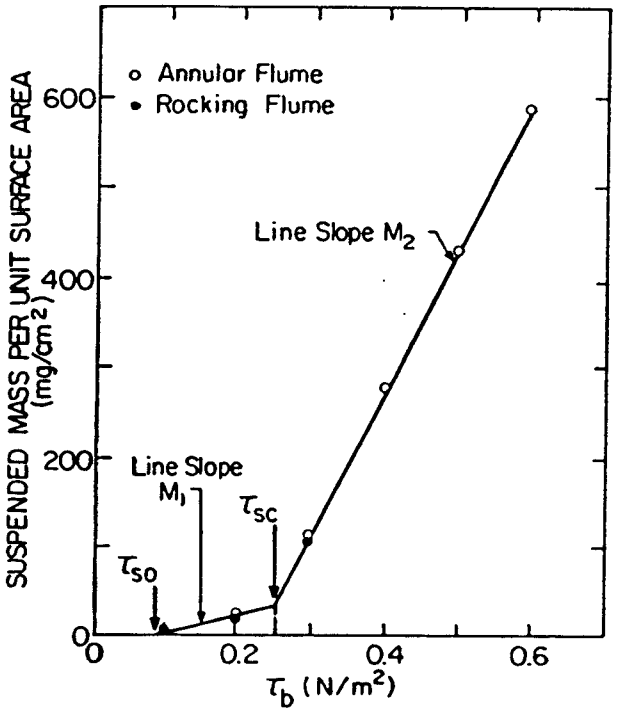

Fig. 21. Mass Per Unit Surface Area versus Shear Stress, Deposited Kaolinite, Both Flumes.

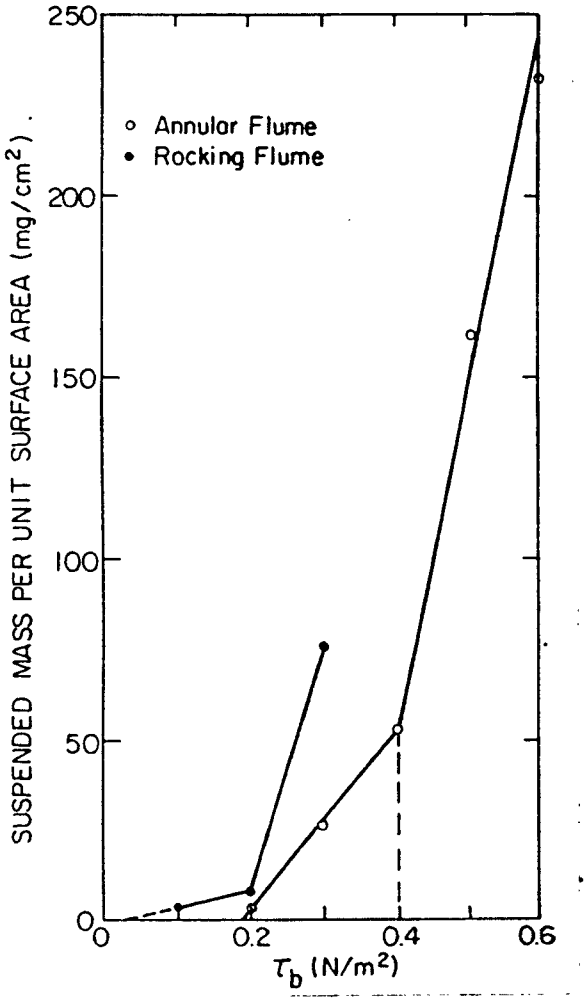

Fig. 22. Mass Per Unit Surface Area versus Shear Stress, Deposited Cedar Key Mud, Both Flumes.

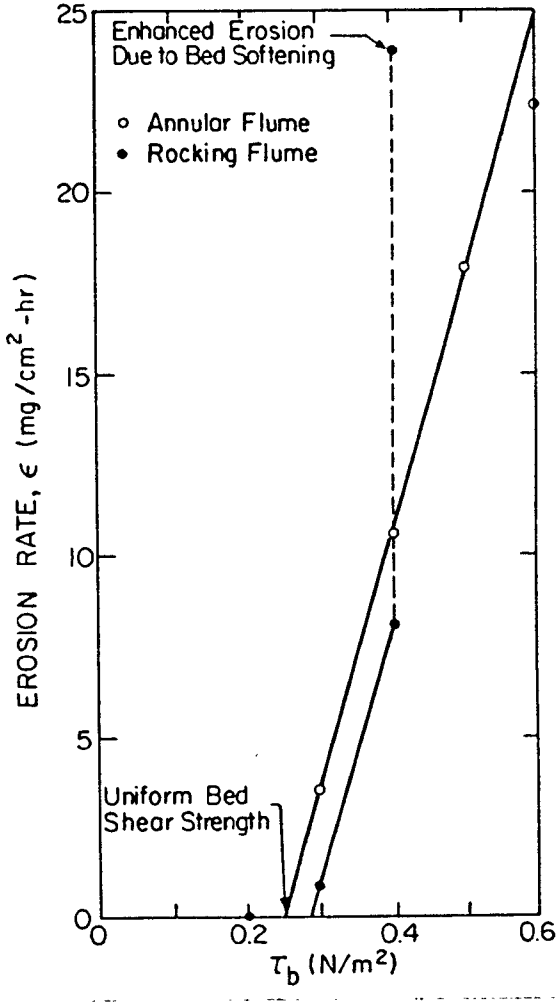

Fig. 23. Erosion Rate versus Shear Stress, Placed Kaolinite, Both Flumes.

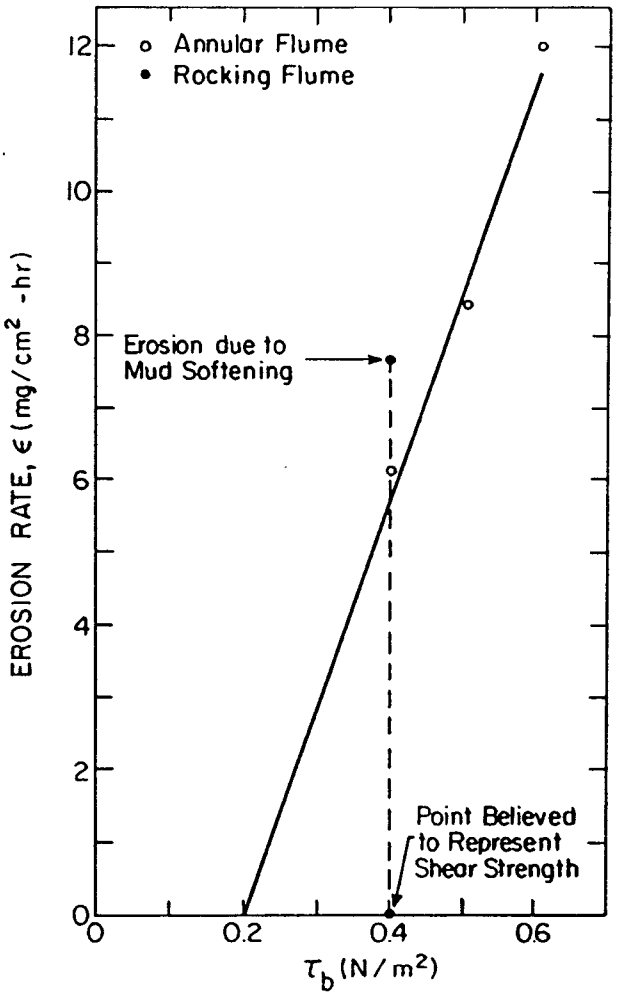

Fig. 24. Erosion Rate versus Shear Stress, Placed Cedar Key Mud, Both Flumes.

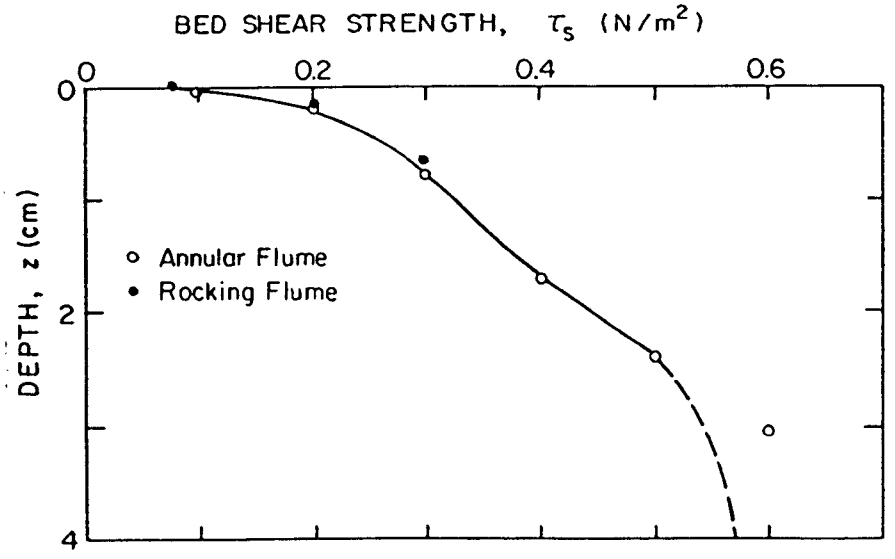

Fig. 25. Variation of Bed Shear Strength with Depth for Deposited Kaolinite, Both Flumes.

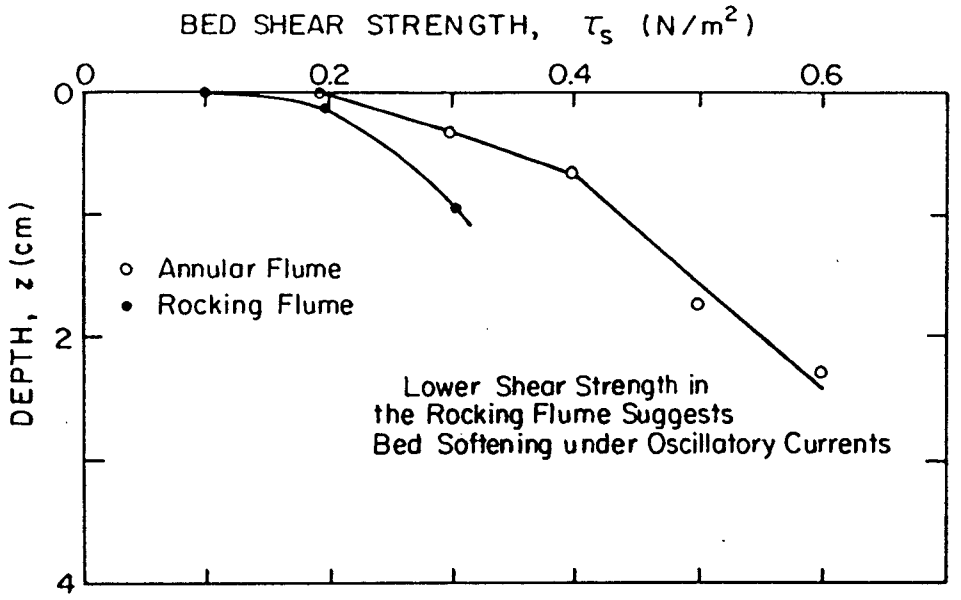

Fig. 26. Variation of Bed Shear Strength with Depth for Deposited Cedar Key Mud, Both Flumes.

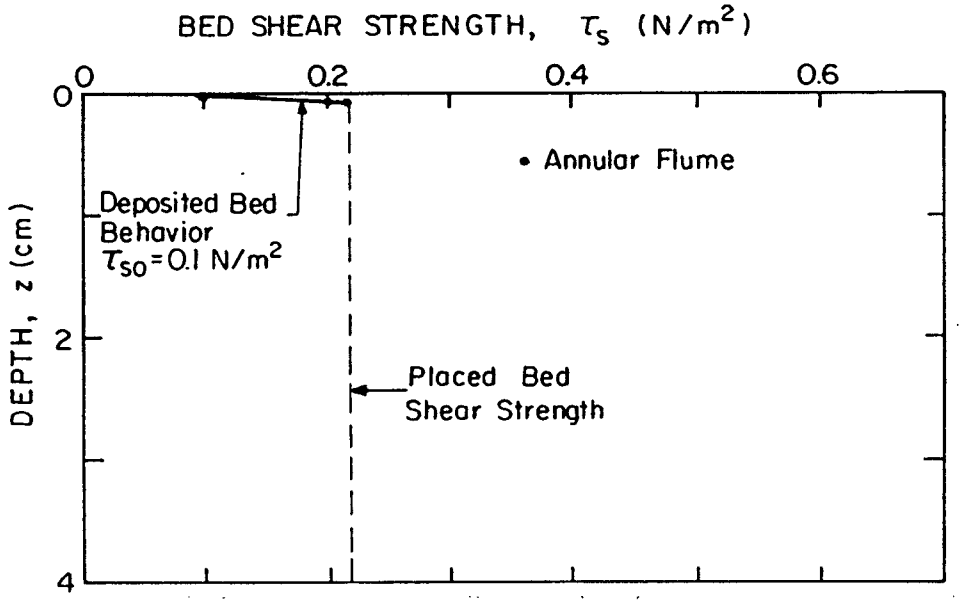

Fig. 27. Variation of Bed Shear Strength with Depth for Placed Cedar Key Mud, Annular Flume.

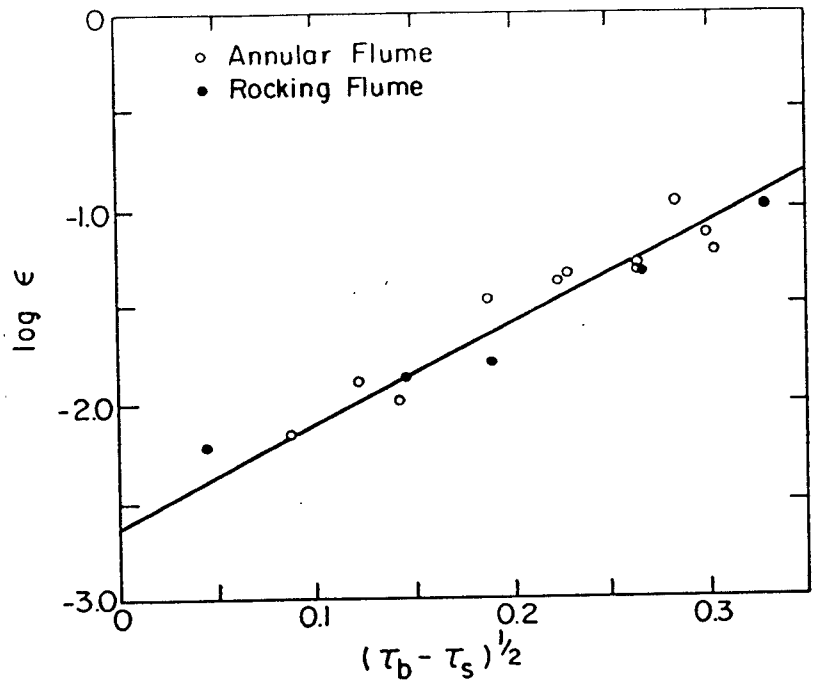

Fig. 28. Log ε versus $(\tau_b - \tau_s)^{0.5}$ for Deposited Kaolinite, Both Flumes.

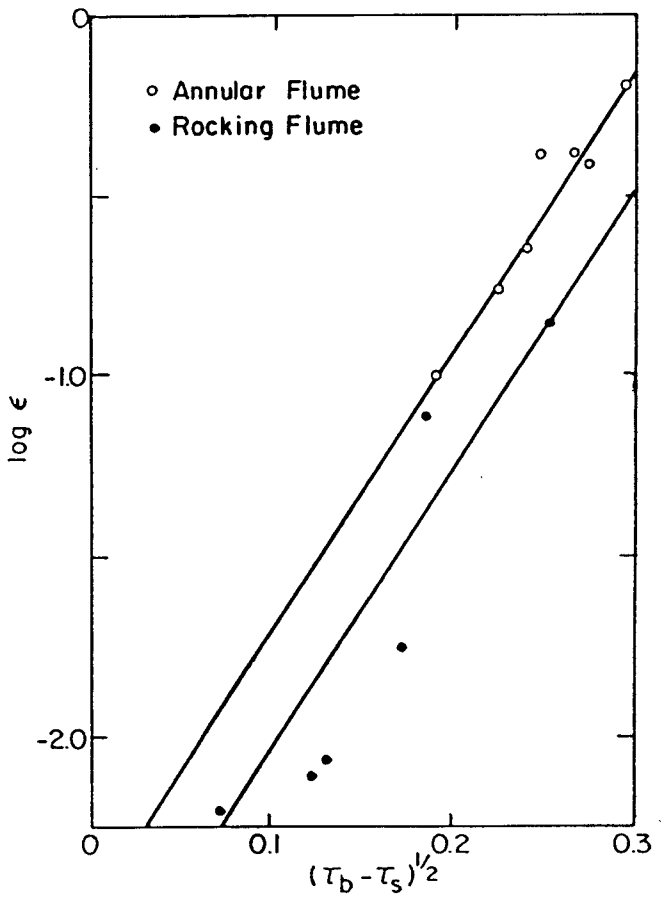

Fig. 29. Log ε versus $(\tau_b - \tau_s)^{0.5}$ for Deposited Cedar Key Mud, Both Flumes.

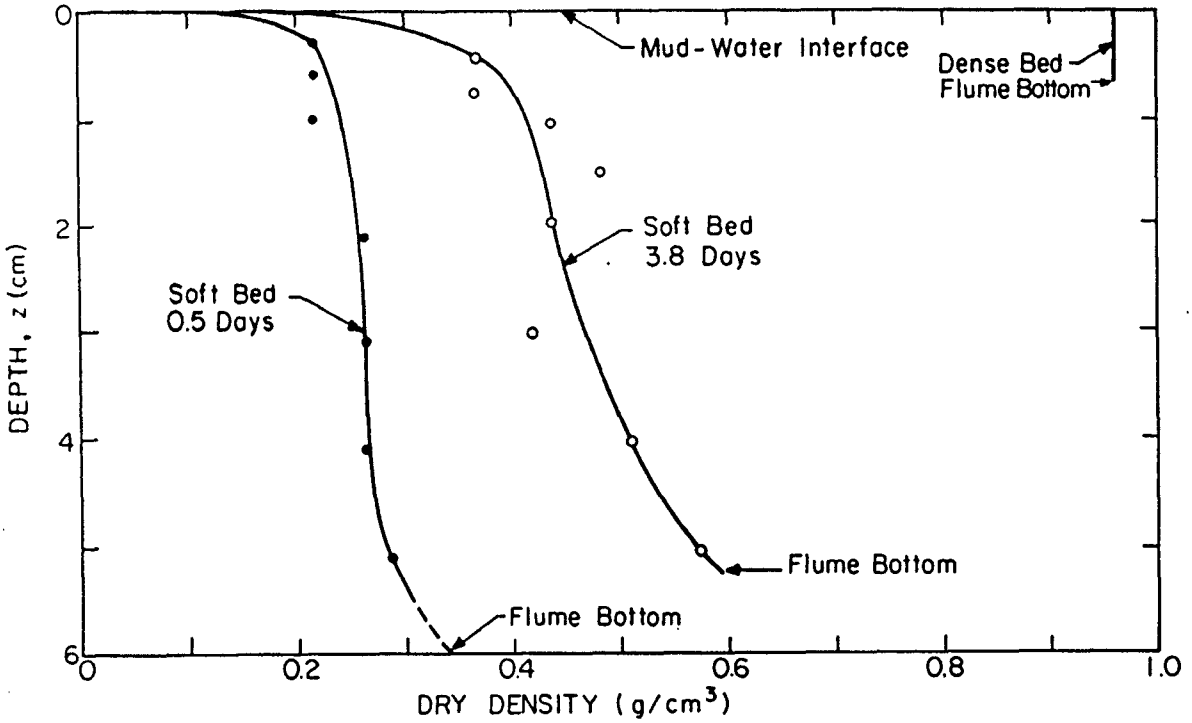

Fig. 30. Bed Dry Density Profiles, Bay Mud.

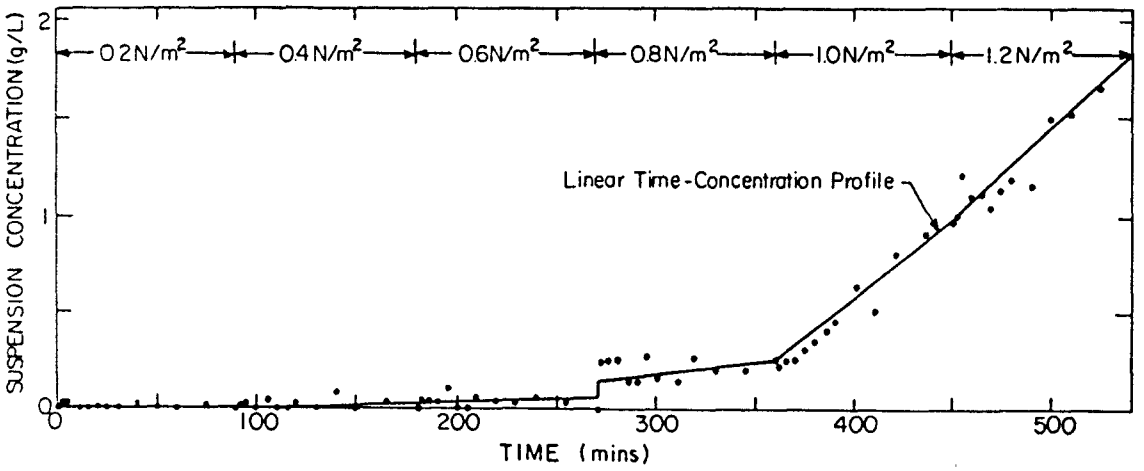

Fig. 31. Time-Concentration Relationship, Bay Mud, Dense Bed, Annular Flume (Test 1).

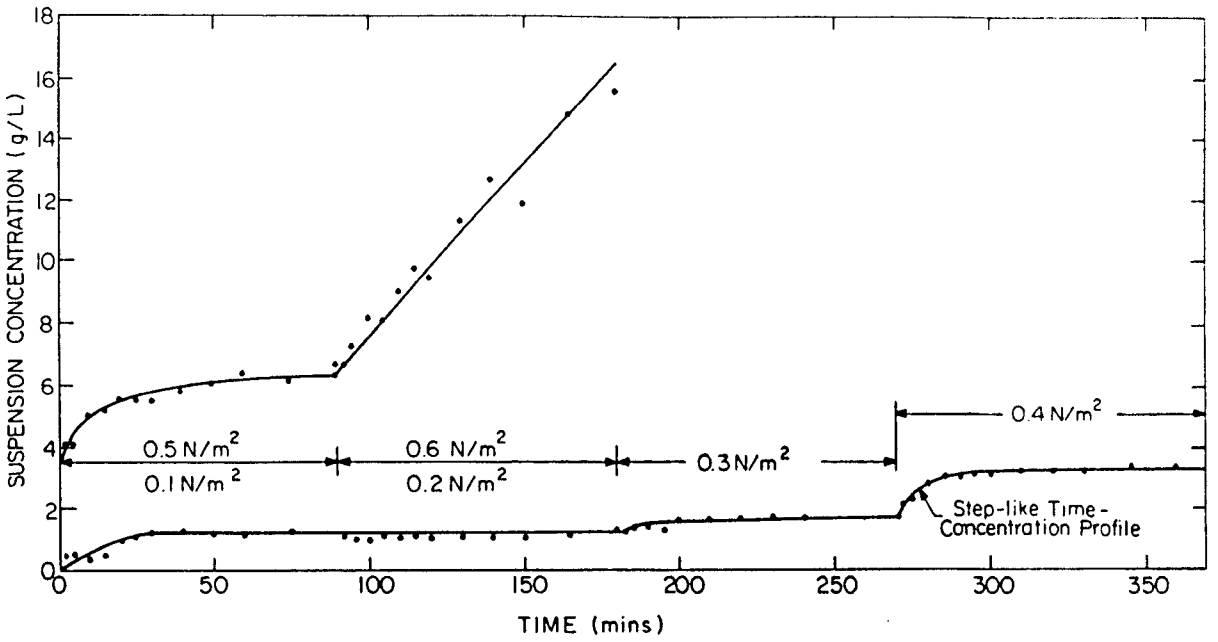

Fig. 32. Time-Concentration Relationship, Bay Mud, Deposited Bed, 0.5 Day Consolidation, Annular Flume (Test 2).

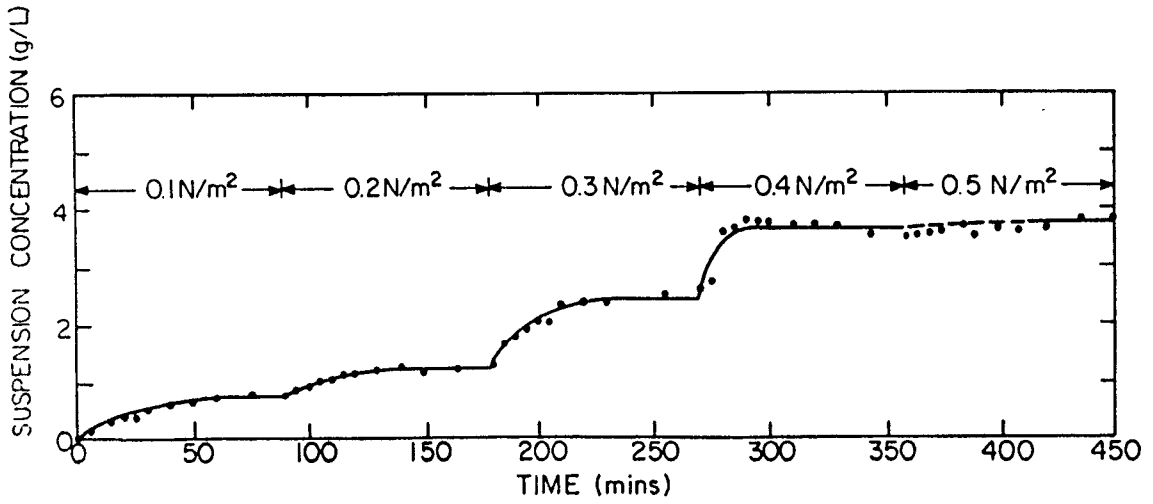

Fig. 33. Time-Concentration Relationship, Bay Mud, Deposited Bed, 0.5 Day Consolidation, Rocking Flume (Test 3).

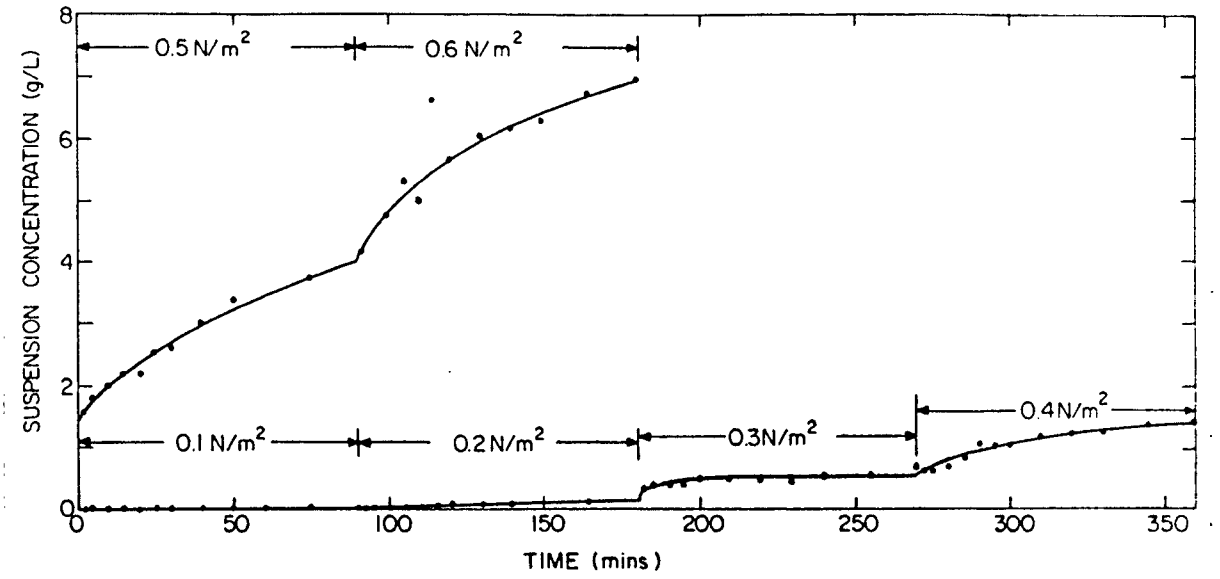

Fig. 34. Time-Concentration Relationship, Bay Mud, Deposited Bed, 3.8 Day Consolidation, Annular Flume (Test 4).

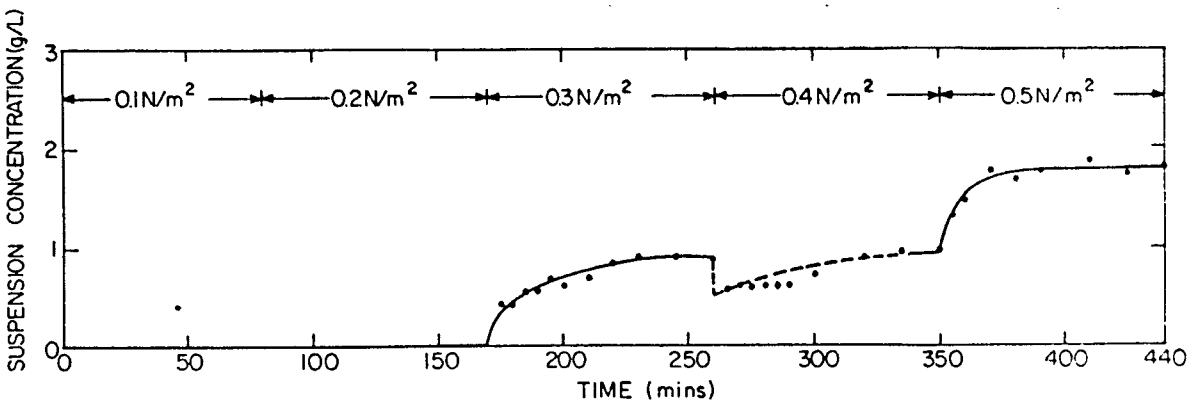

Fig. 35. Time-Concentration Relationship, Bay Mud, Deposited Bed, 3.8 Day Consolidation, Rocking Flume (Test 5).

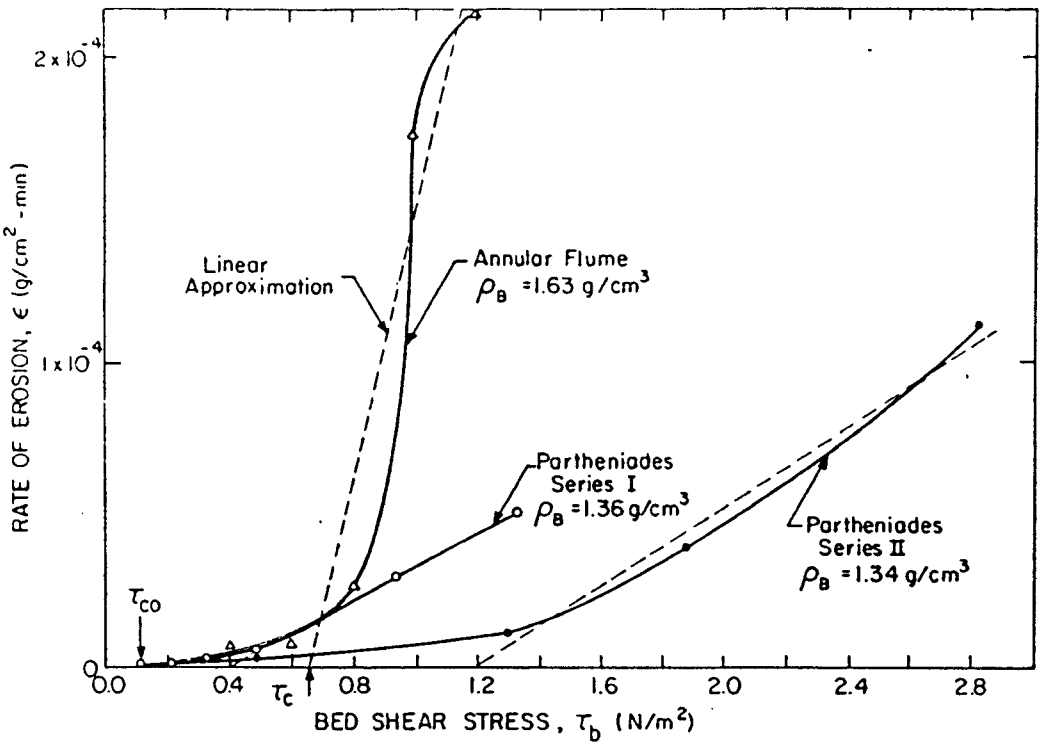

Fig. 36. Rate of Erosion versus Bed Shear Stress, Bay Mud, Dense Bed and Results of Partheniades.

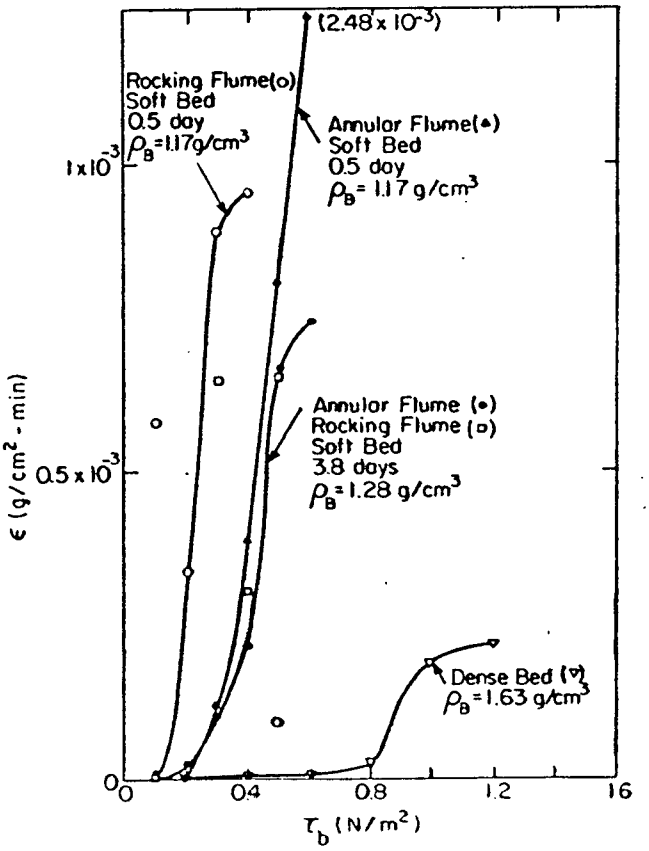

Fig. 37. Rate of Erosion versus Bed Shear Stress, Bay Mud, Dense Bed and Soft Beds.

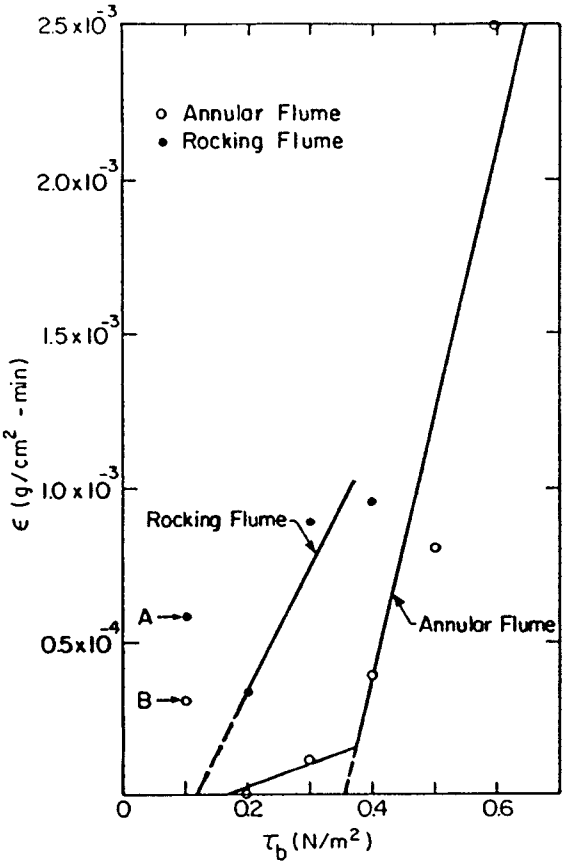

Fig. 38. Rate of Erosion versus Bed Shear Stress, Bay Mud, Soft Beds, 0.5 Day Consolidation.

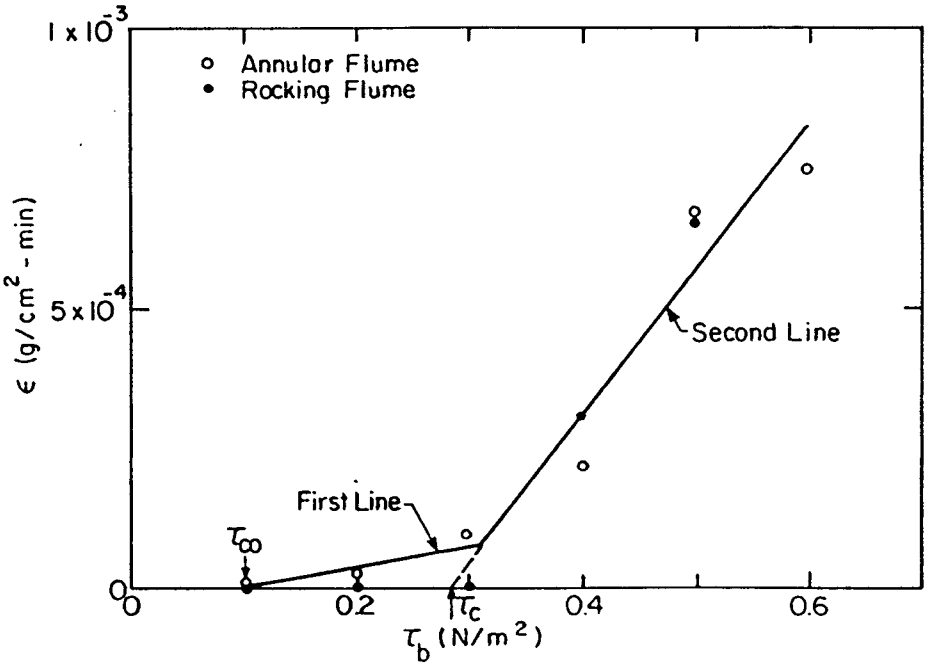

Fig. 39. Rate of Erosion versus Bed Shear Stress, Bay Mud, Soft Beds, 3.8 Day Consolidation.

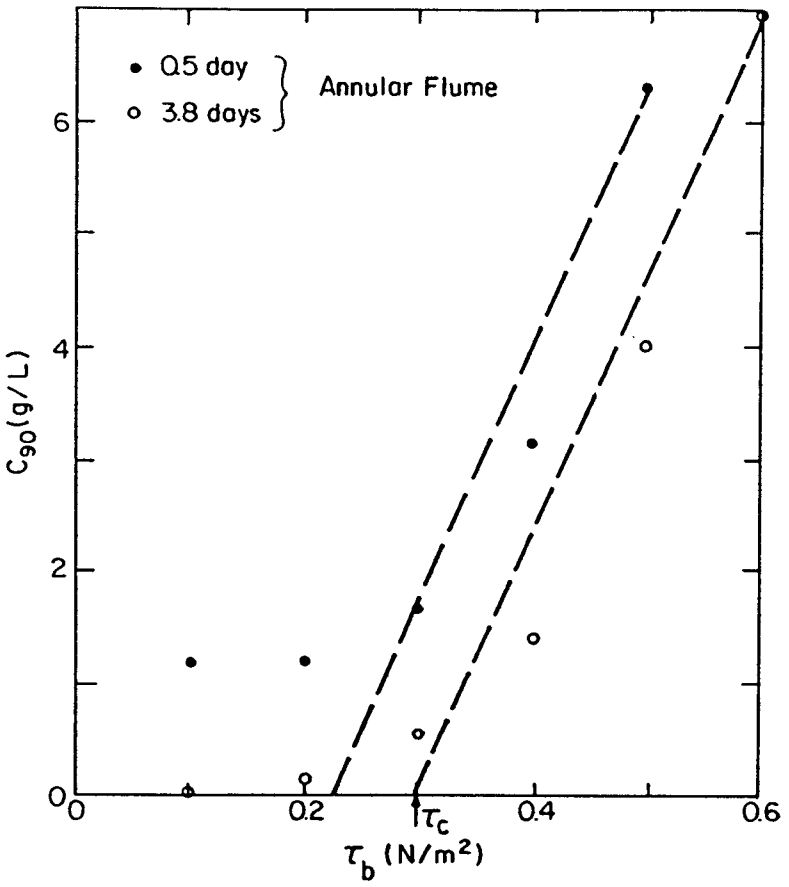

Fig. 40. Final Concentration, C_{90}, versus Bed Shear Stress, τ_b, Bay Mud, Soft Beds, Annular Flume.

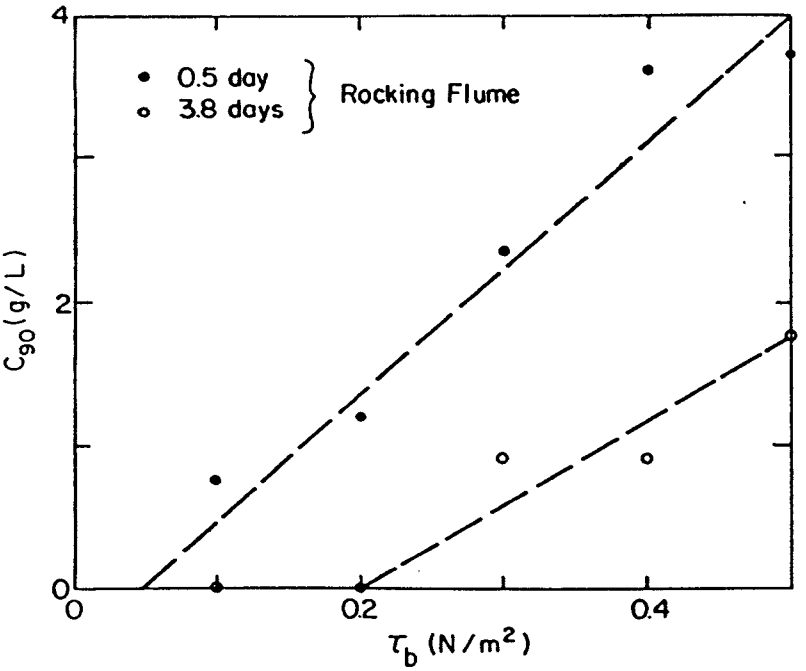

Fig. 41. Final Concentration, C_{90}, versus Bed Shear Stress, τ_b, Bay Mud, Soft Beds, Rocking Flume.

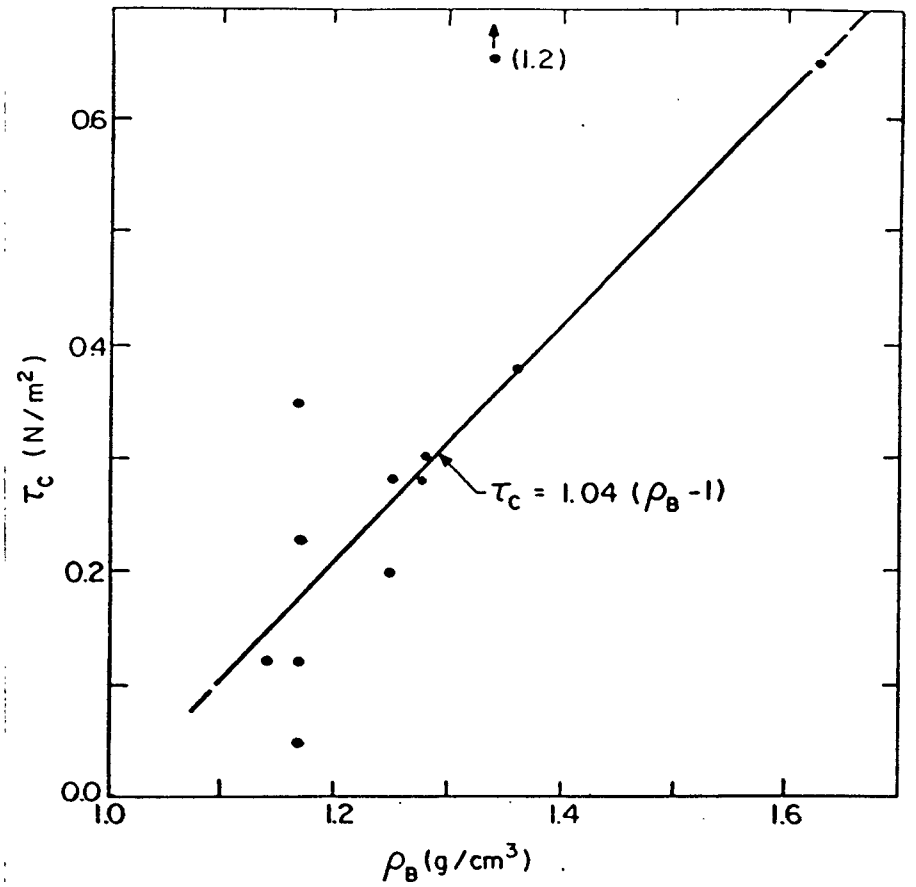

Fig. 42. Critical Shear Stress, τ_c, as a Function of Bed Bulk Density, ρ_B, Bay Mud.

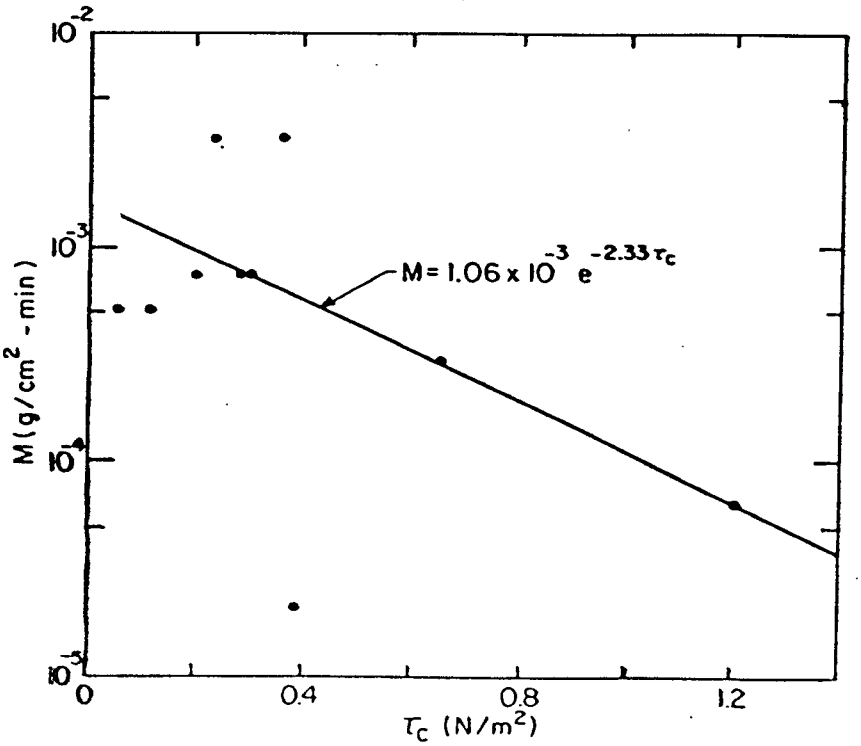

Fig. 43. Erosion Rate Constant, M, as a Function of Critical Shear Stress, τ_c, Bay Mud.

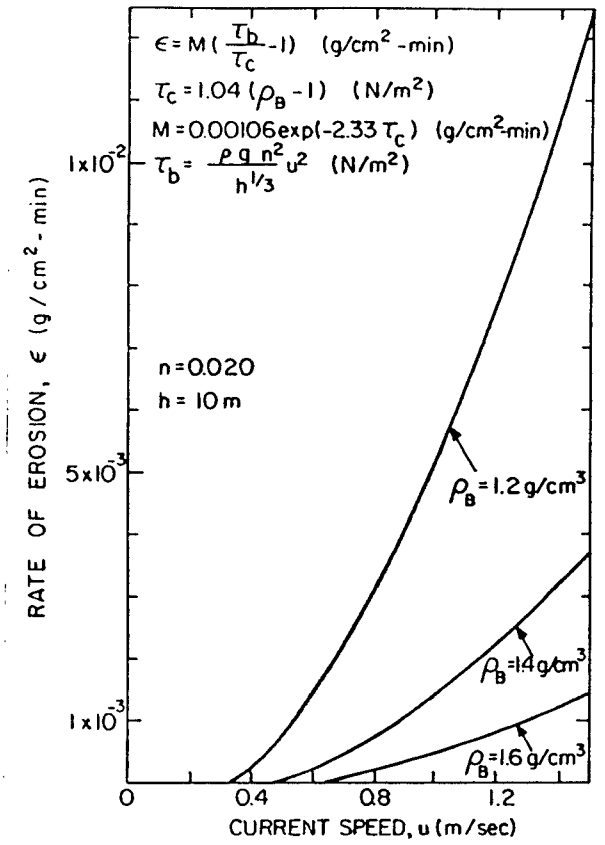

Fig. 44. Erosion Rate Dependence on Bed Bulk Density and Current Speed, Bay Mud.

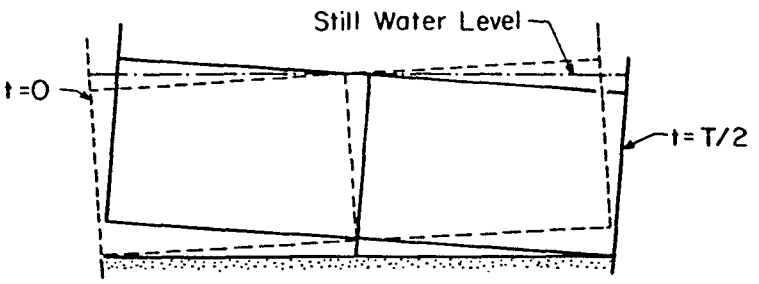

Fig. A.1. Oscillatory Motion of the Rocking Flume.

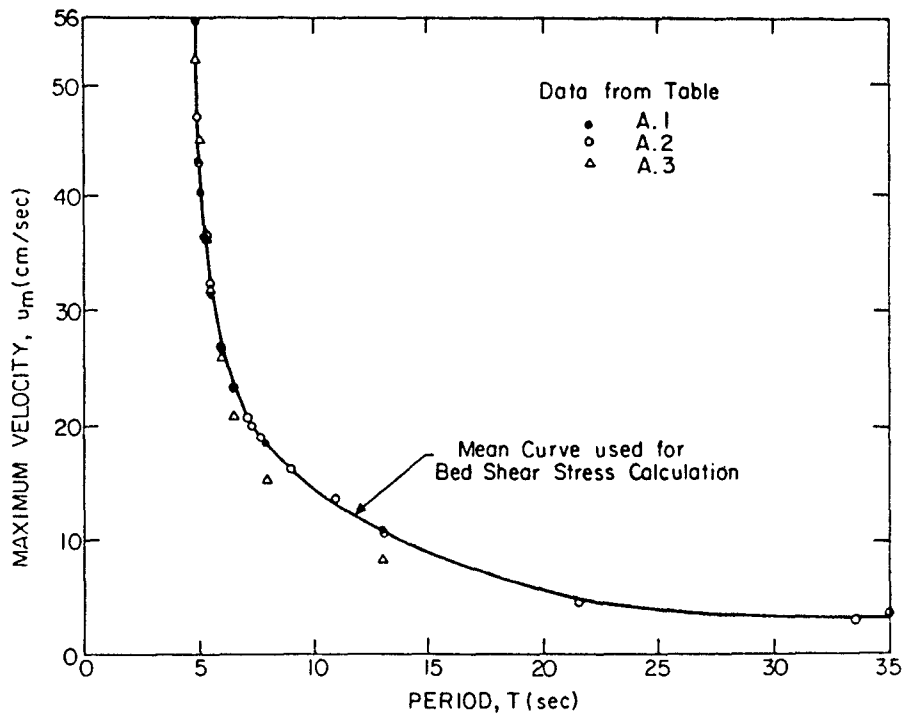

Fig. A.2. Calibration Curve between Maximum Velocity, u_m, and Wave Period, T, in the Rocking Flume.

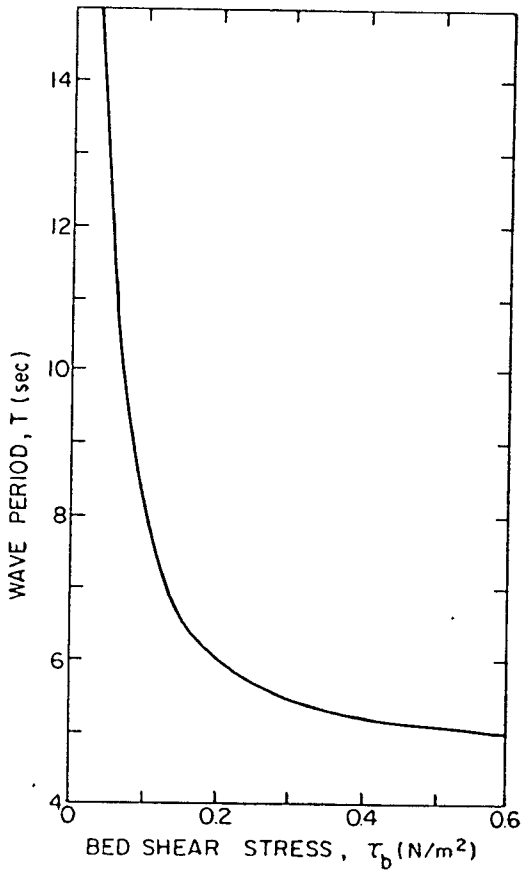

Fig. A.3. Calibration Curve between Bed Shear Stress, τ_b, and Wave Period, T, in the Rocking Flume.